Cellular/Molecular

Phosphorylated CCAAT/Enhancer Binding Protein β Contributes to Rat HIV-Related Neuropathic Pain: *In Vitro* and *In Vivo* Studies

Hyun Yi, Shue Liu, Yuta Kashiwagi, Daigo Ikegami, Wan Huang, Hirotsugu Kanda, Takafumi Iida, Ching-Hang Liu, Keiya Takahashi, David A. Lubarsky, and Shuanglin Hao

Department of Anesthesiology, University of Miami Miller School of Medicine, Miami, Florida 33136

Chronic pain is increasingly recognized as an important comorbidity of HIV-infected patients, however, the exact molecular mechanisms of HIV-related pain are still elusive. CCAAT/enhancer binding proteins (C/EBPs) are expressed in various tissues, including the CNS. C/EBPβ, one of the C/EBPs, is involved in the progression of HIV/AIDS, but the exact role of C/EBPβ and its upstream factors are not clear in HIV pain state. Here, we used a neuropathic pain model of perineural HIV envelope glycoprotein gp120 application onto the rat sciatic nerve to test the role of phosphorylated C/EBPβ (pC/EBPβ) and its upstream pathway in the spinal cord dorsal horn (SCDH). HIV gp120 induced overexpression of pC/EBPβ in the ipsilateral SCDH compared with contralateral SCDH. Inhibition of C/EBPβ using siRNA against C/EBPβ reduced mechanical allodynia. HIV gp120 also increased TNFα, TNFRI, mitochondrial superoxide ($mtO_2^{\cdot-}$), and pCREB in the ipsilateral SCDH. ChIP-qPCR assay showed that pCREB enrichment on the C/EBPβ gene promoter regions in rats with gp120 was higher than that in sham rats. Intrathecal TNF soluble receptor I (functionally blocking TNFα bioactivity) or knockdown of TNFRI using antisense oligodeoxynucleotide against TNFRI reduced mechanical allodynia, and decreased $mtO_2^{\cdot-}$, pCREB and pC/EBPβ. Intrathecal Mito-tempol (a mitochondria-targeted $O_2^{\cdot-}$ scavenger) reduced mechanical allodynia and decreased pCREB and pC/EBPβ. Knockdown of CREB with antisense oligodeoxynucleotide against CREB reduced mechanical allodynia and lowered pC/EBPβ. These results suggested that the pathway of TNFα/TNFRI–$mtO_2^{\cdot-}$–pCREB triggers pC/EBPβ in the HIV gp120-induced neuropathic pain state. Furthermore, we confirmed the pathway using both cultured neurons treated with recombinant TNFα *in vitro* and repeated intrathecal injection of recombinant TNFα in naive rats. This finding provides new insights in the understanding of the HIV neuropathic pain mechanisms and treatment.

Key words: epigenetics; HIV pain; mitochondrial superoxide; pC/EBPβ; pCREB; TNFα

Significance Statement

Painful HIV-associated sensory neuropathy is a neurological complication of HIV infection. Phosphorylated C/EBPβ (pC/EBPβ) influences AIDS progression, but it is still not clear about the exact role of pC/EBPβ and the detailed upstream factors of pC/EBPβ in HIV-related pain. In a neuropathic pain model of perineural HIV gp120 application onto the sciatic nerve, we found that pC/EBPβ was triggered by TNFα/TNFRI–$mtO_2^{\cdot-}$–pCREB signaling pathway. The pathway was confirmed by using cultured neurons treated with recombinant TNFα *in vitro*, and by repeated intrathecal injection of recombinant TNFα in naive rats. The present results revealed the functional significance of TNFα/TNFRI–$mtO_2^{\cdot-}$–pCREB–pC/EBPβ signaling in HIV neuropathic pain, and should help in the development of more specific treatments for neuropathic pain.

Introduction

Since 1996, highly active antiretroviral therapy (HAART) has changed HIV infection from an inevitably fatal disease to a complex, chronic infection, allowing patients with HIV to achieve near-normal life expectancy (Samji et al., 2013). However, they often suffer from high rates of medical and psychiatric comor-

Received Nov. 27, 2016; revised Nov. 1, 2017; accepted Nov. 13, 2017.

Author contributions: H.Y., S.L., D.I., W.H., H.K., T.I., C.-H.L., and S.H. designed research; H.Y., S.L., Y.K., D.I., W.H., H.K., T.I., C.-H.L., K.T., and S.H. performed research; H.Y., S.L., D.I., W.H., H.K., T.I., C.-H.L., and S.H. analyzed data; H.Y., D.I., D.A.L., and S.H. wrote the paper.

This work was supported by Grants from the U.S. National Institutes of Health NS066792 (S.H.) and DA34749 (S.H.), and by the Department of Anesthesiology, University of Miami Miller School of Medicine, Miami, FL. We thank Dr. Joy Joseph (Biophysics Department, Medical College of Wisconsin) for providing Mito-Tempol as gift, Dr. Stephen Koslow (NIH) for checking the paper, and Dr. Frank Porreca (University of Arizona) for review of the paper.

The authors declare no competing financial interests.

Correspondence should be addressed to Dr. Shuanglin Hao, Department of Anesthesiology, University of Miami Miller School of Medicine, Miami, FL 33136. E-mail: shao@med.miami.edu.

DOI:10.1523/JNEUROSCI.3647-16.2017

Copyright © 2018 the authors 0270-6474/18/380555-20$15.00/0

bidities. In a clinical report, most (80.6%) of the HIV patients had an undetectable viral load and near half of these patients (48.7%) reported pain (Merlin et al., 2012). HIV-associated sensory neuropathy (HIV-SN) is one of common forms of neuropathies (Keswani et al., 2002; Höke and Cornblath, 2004; Nath, 2015). Painful HIV-SN is a neurological complication of HIV infection (Cherry et al., 2012; Nath, 2015). Despite better viral control in the antiretroviral therapy (ART) era, the virus persists in a small number of cells that are refractory to this treatment and are not detected. The continued prevalence of painful HIV-SN may reflect subsequent chronic inflammation that are below the level of detection and yet sufficient to cause neurotoxicity (Kranick and Nath, 2012). CCAAT/enhancer binding proteins (C/EBPs; a family of transcription factors) are expressed in various tissues, playing a role in inflammatory response, synaptic plasticity, and memory (Taubenfeld et al., 2001; Alberini, 2009; Jiang et al., 2017). C/EBPβ mRNA (a member of the C/EBPs family) is elevated in the brain of HIV-1 encephalitis patients (Fields et al., 2011). Recent studies shows that C/EBPβ is an endogenous initiator of neuropathic pain and could be a potential target for the prevention and treatment of this disorder (Li et al., 2017). Phosphorylated C/EBPβ (pC/EBPβ) may influence AIDS progression (Mameli et al., 2007), but it is not clear whether pC/EBPβ is involved and what triggers pC/EBPβ in the HIV gp120-related pain model.

We have reported that perineural HIV gp120 application onto the sciatic nerve increases glial tumor necrosis factor α (TNFα) expression in the ipsilateral spinal cord dorsal horn (SCDH; Zheng et al., 2011, 2014; Huang et al., 2014). HIV patients with chronic pain show an increased TNFα in the spinal cord (Shi et al., 2012; Yuan et al., 2014). Reactive oxygen species (ROS) accumulation has been observed in the mitochondria of the SCDH neurons in different pain models (Schwartz et al., 2009; Kim et al., 2011; Salvemini et al., 2011). Mitochondrial ROS (mtROS) signaling events play an important role in the pathogenesis of chronic pain (Sui et al., 2013) and HIV pain model in rats (Kanao et al., 2015; Iida et al., 2016). The induction of cAMP response element binding protein (CREB) phosphorylation in spinal cord slices is in response to C-fiber stimulation, which mediates transcriptional regulation in the dorsal horn neurons (Kawasaki et al., 2004). Phosphorylated CREB (pCREB) results in long-lasting synaptic plasticity (Nestler, 2002; Hagiwara et al., 2009), and pCREB is upregulated in the SCDH of pain-positive HIV patients (Shi et al., 2012). HIV gp120 triggers neurotoxicity, oxidant injury, and neuroinflammation (Yuan et al., 2014; Hoefer et al., 2015; Nath, 2015; Kanda et al., 2016b; Meeker et al., 2016). Here, we demonstrated that pC/EBPβ was triggered by TNFα/TNFRI, mitochondrial superoxide ($mtO_2^{\cdot-}$)–pCREB pathway in the gp120 neuropathic pain state. Meanwhile, we verified that pC/EBPβ can be directly stimulated by TNFα via ROS and pCREB in both cultured neuronal cells and naive rats.

Materials and Methods

Animals and perineural gp120 neuropathic pain model. The model of perineural gp120 neuropathic pain in rats was reported (Herzberg and Sagen, 2001). In the present studies, male Sprague-Dawley rats weighing 225–250 g (Charles River Laboratories; RRID:RGD_737891) were housed one to three per cage ~7 d before the beginning of all studies. All housing conditions and every experimental procedure including the power analysis were approved by the University Animal Care and Use Committee. Under anesthesia, the rat left sciatic nerve was exposed in the popliteal fossa. A 2 × 6 mm strip of oxidized regenerated cellulose was previously soaked in 250 μl of a 0.1% rat serum albumin (RSA) in saline, containing 400 ng of gp120MN (cat#1021, Immunodiagnostics.) or 0.1% RSA in saline for sham surgery (Herzberg and Sagen, 2001; Wallace et al., 2007a). Animals showing motor deficits or 85% of body weight loss after implantation were excluded. Animals were assigned to experimental groups randomly. Less than 5% of rats with gp120 application showed motor deficits or body weight loss, and those were excluded from the studies. Experienced researchers performed the surgery.

Mechanical threshold. Mechanical withdrawal threshold was determined using calibrated von Frey filaments (Stoelting) introduced serially to the ipsilateral hindpaw in ascending order of strength. Animals were placed in nontransparent plastic cubicles on a mesh floor for an acclimatization period of at least 30 min in the morning of the test day. A series of 10 calibrated fine von Frey filaments (0.4, 0.7, 1.2, 1.5, 2.0, 3.6, 5.5, 8.5, 11.8, and 15.1 g) was presented serially to the gp120 application hindpaw in ascending order of strength with sufficient force to cause slight bending against the paw and held for 6 s. A positive response was defined as a rapid withdrawal and/or licking of the paw immediately on application of the stimulus. Whenever there was a positive response to a stimulus, the next smaller von Frey hair was applied, and whenever there was a negative response, the next higher force was applied. In the absence of a response at a pressure of 15.1 g, animals were assigned to this cutoff value. Mechanical withdrawal threshold was determined according to the method described previously with a tactile stimulus producing a 50% likelihood of withdrawal determined by using the up-and-down method (Chaplan et al., 1994; Iida et al., 2016). Experimenters were blind to the group treatment during behavioral test.

Intrathecal catheter implantation. For intrathecal administration of drugs, an intrathecal catheter was implanted under isoflurane anesthesia as previously described (Zheng et al., 2011). Briefly, through an incision in the atlanto-occipital membrane, a polyethylene (PE-10) catheter, filled with 0.9% saline, was advanced 8.5 cm caudally to position its tip at the level of the lumbar enlargement. The rostral tip of the catheter was passed subcutaneously, externalized on top of the skull, and sealed with a stainless steel plug. Animals showing neurological deficits after implantation were excluded. Animals were used within 5 d after implantation of the catheter.

Repeatedly intrathecal injection of TNFα. To induce pain-like behavior, recombinant rat TNFα (rTNFα; catalog #400-14, PeproTech) was prepared. Saline or rTNFα (0.3 ng) 10 μl was intrathecally injected (twice daily at 10:00 A.M. and 6:00 P.M.) for 2 d. Sixteen hours (day 3) after the fourth injection, mechanical threshold was examined using von Frey filaments.

Cultured neuronal cells treated with rTNFα. The rat neuronal cell line (B35, CRL-2754; RRID:CVCL_1951) was obtained from American Type Culture Collection. Cells were treated with rTNFα (2 ng/ml; Peprotech) or saline (vehicle as control) for 3 h for neurochemical analysis. For Western blots, the cells were plated in a 6-well plate and treated with rTNFα or vehicle for 3 h, collected, and stored at −80°C for further analysis. For Mito-Tempol (Mito-T; a mitochondria-targeted $O_2^{\cdot-}$ scavenger) treatment, the cells were pretreated with 100 μM Mito-T (100 μM; Liang et al., 2014) or vehicle for 1 h before rTNFα, and incubated an additional 3 h.

Quantitative RT-PCR. B35 cells or the SCDH tissue of rat samples of ipsilateral side to gp120 application was collected, and total RNA was isolated with RNeasy mini kit (catalog #74104, Qiagen). The RNA sample was treated with DNase I on column to remove genomic DNA. One microgram of RNA was converted into cDNA using Superscript VILO master mix (catalog #11755-050, Invitrogen), and then real time PCR was performed with Fast SYBR green master mix (catalog #4385612, Applied Biosystems). For real-time PCR, the following primers were used: C/EBPβ forward 5′-GGTTTCGGGACTTGATGCAA-3′ and reverse 5′-ACCCCGCAGGAACATCTTTA-3′; and GAPDH forward 5′-CAGGGCTGCCTTCTCTTGTG-3′ and reverse 5′-AACTTGCCGTGG GTAGAGTC-3′. Specificity of the PCR product was confirmed by running agarose gel electrophoresis. All reaction data were calculated with $2^{-\Delta\Delta Ct}$ values and normalized with GAPDH.

Western blots. Under deep anesthesia with isoflurane, the L4-5 dorsal horn ipsilateral to gp120 application was removed rapidly, frozen on dry ice, and stored at −80°C. B35 cells or SCDH tissue was homogenized and lysed with 1× RIPA protein lysis buffer containing protease and phosphatase inhibitor cocktail 2 and 3 (catalog #P8340, P5726, P0044, Sigma-

Aldrich) as previously described (Zheng et al., 2012). The protein concentration of tissue lysates was determined with a BCA Protein Assay Kit (Pierce Biotechnology). Proteins (30 μg) denatured, and loaded on to 10% SDS-PAGE gel, and transferred onto a PVDF membrane. The membrane was incubated with primary antibodies overnight at 4°C, including rabbit polyclonal anti-pC/EBPβ (1:250; catalog #sc-16994-R, Santa Cruz Biotechnology; RRID:AB_2078179), rabbit polyclonal anti-C/EBPβ(1:10,000; sc-150x, Santa Cruz Biotechnology; RRID:AB_2260363), rabbit polyclonal anti-TNFα (1:1000; catalog #AB1837P, Millipore; RRID:AB_2204499), mouse monoclonal anti-TNF-RI(1:1000; catalog #sc-8436, Santa Cruz Biotechnology), mouse monoclonal anti-pCREB (1:1000; catalog #05-807, Millipore; RRID:AB_310017), and rabbit polyclonal anti-CREB(1:1000; catalog #sc-186, Santa Cruz Biotechnology; RRID:AB_2086021). For loading control, the blots were probed with β actin antibody (mouse monoclonal anti-β-actin (1:8000; catalog #A5441, Sigma-Aldrich; RRID:AB_476744). The membrane was incubated with secondary antibodies at room temperature, and then developed in chemiluminescence solution (catalog #34076, Pierce Biotechnology). Chemiluminescence values from targeted band intensity was analyzed, quantified, and normalized with β-actin using a ChemiDoc imaging system (Bio-Rad).

Chromatin immunoprecipitation with quantitative PCR . For B35 cells 3 h after treatment with rTNFα, cells were collected; vehicle treatment (saline) was used for control. In *in vivo* studies, 2 weeks after gp120 application the spinal cords were harvested. Animals in the sham group received vehicle application (1% RSA) as control. Both B35 cells and spinal cord tissues were homogenized and fixed with 1% paraformaldehyde (PFA) for 10 min. Then, 2.5 M glycine was added to stop the reaction. Fixed cells were washed with cold PBS with phosphatase inhibitor cocktail (catalog #P8340, Sigma-Aldrich), and samples were resuspended with 250 μl of SDS lysis buffer (50 mM Tris-HCl, pH8.0, 10 mM EDTA, 1% SDS). Samples were sonicated to shear the chromatin to the size of 200–1000 bp length. Size of the sheared chromatin was confirmed by running 1.5% agarose gel. Ten microliters from the supernatant was taken as "input" and save it at −20°C. For immunoprecipitation, 15 μg of sonicated chromatin was diluted in 0.5 ml chromatin immunoprecipitation (ChIP) dilution buffer (1.1%w/v DOC, 1.1%w/v Triton X-100, 167 mM NaCl, 50 mM Tris-HCl pH8.0), and then ChIP-validated antibody, pCREB (catalog #sc-7978, Santa Cruz Biotechnology; RRID:AB_2086020) was added to each sample. Samples were incubated overnight at 4°C with gentle rotation, following which 20 μl protein G magnetic beads (catalog #88848, Life Technologies) were added and incubated additional 2 h at 4°C. After few washes, both immunoprecipitated and input samples were incubated with Proteinase K (catalog #P2308, Sigma-Aldrich) at 62°C for 2 h to free DNA. DNA was purified using Gene Elute PCR cleanup kit (catalog #NA1020, Sigma-Aldrich). Immunoprecipitated and input DNA were analyzed by quantitative PCR analysis with SYBR Green. The primers of C/EBPβ promoter for ChIP were used to amplify the segment including the CRE sites (Zhang et al., 2004; Pulido-Salgado et al., 2015), forward, 5′-CCAGGACACCGCTCAGTAT-3′, reverse, 5′-CCGAGCGGGAGGTTTATAAGG-3′. Specificity of qPCR was verified with melting curve analysis and running on agarose gel electrophoresis. All reaction data were calculated with $2^{-\Delta\Delta Ct}$ values, and the value of pCREB immunoprecipitated DNA was calculated as a percentage of the value of input control; the final values were normalized to ratio of sham or saline group (Imai et al., 2013; Heller et al., 2016).

Immunohistochemistry. Two weeks after gp120, the animals were perfused with 4% paraformaldehyde in 0.1 m PBS. The spinal cord was postfixed and cryoprotected. Immunostaining of GFAP, OX42, NeuN, pC/EBPβ, TNFRI, and pCREB in the SCDH was performed as described previously (Hao et al., 2011). Briefly, the cryosections of the spinal cord were probed with mouse anti-GFAP polyclonal antibody (1:2000; catalog #G3893, Sigma-Aldrich; RRID:AB_477010), mouse anti-OX42 (1:200; catalog #CBL1512, Millipore Bioscience Research Reagents; RRID:AB_93253), mouse anti-NeuN monoclonal antibody (A60; 1:500; catalog #MAB377, Millipore Bioscience Research Reagents; RRID:AB_2298772), rabbit anti-NeuN (1:2000; catalog #ABN78, Millipore; RRID:AB_10807945), rabbit anti-pC/EBPβ (1:200; catalog #sc-16994-R, Santa Cruz Biotechnology; RRID:AB_2078179), mouse anti-TNFRI (1:100; sc-8436, Santa Cruz Biotechnology; RRID:AB_628377), and mouse anti-pCREB (1:200; catalog #05–807, Millipore; RRID:AB-310017). These treatments were then followed by complementary secondary antibodies labeled with green-fluorescent AlexaFluor 488, or red-fluorescent AlexaFluor 594 (1:2000; Invitrogen), 2 h at room temperature. Fluorescence images were captured by a fluorescent microscopy (Fluorescent M Leica/Micro CDMI 6000B).

Detection of $mtO_2^{\cdot-}$ production. MitoSox Red reagent (catalog #M36008, Invitrogen) is readily oxidized by superoxide, producing red fluorescence oxidation product. For $mtO_2^{\cdot-}$ images in the SCDH in rats, MitoSox was prepared as described previously (Schwartz et al., 2009; Kanao et al., 2015). MitoSox Red was dissolved in a 1:1 mixture of dimethylsulfoxide and saline to a final concentration of 33 μM. Approximately 70 min after intrathecal injection of MitoSox (30 μl), rats were perfused with 4% paraformaldehyde in 0.1 M PBS. The spinal cord was postfixed 4–15 h in the perfusion fixative, equilibrated in 30% sucrose, cryosectioned at 35 μm, and mounted on gelatin-coated slides. The sections were randomly examined under a fluorescent microscope with a rhodamine filter. Two different regions of the SCDH were photographed from four to five randomly selected sections from each animal: the lateral part of lamina I–II and lamina III–V. The number of MitoSox-positive cellular profiles with distinctive nuclei (dark oval shaped space surrounded by red granules) was counted by an experimenter blind to the condition as previously described (Schwartz et al., 2008, 2009).

To detect $mtO_2^{\cdot-}$ production in the cultured neuronal cells MitoSox Red staining was used as described previously (Ahmed et al., 2012). Cells were stained with 2.5 μM MitoSox in live cell imaging solution for 30 min at 37°C in the dark (Ahmed et al., 2012). The integrated fluorescence density from an entire image was measured and calculated with NIH ImageJ software (RRID:SCR_003070). The average of intensity of MitoSox Red fluorescence was normalized with that in PBS (control) treated cells.

Drugs. The chemicals used in this study were as follows: Both recombinant human TNF soluble receptor I (catalog #310-07; RRID:AB_2665386) and recombinant rat TNFα (catalog #400-14; RRID:AB_2665385) were purchased from PeproTech and dissolved in saline. Mito-T is gift from Dr. Joy Joseph, Biophysics Department, Medical College of Wisconsin. The sequences of rat TNFRI antisense oligodeoxynucleotides (ODNs; Lee et al., 2009), 5′-ACACGGTGTTCTGTTTCTCC-3′, mismatch ODN (mmODN), 5′-ACCCGTTGTTCGGTTGCTCC-3′ were synthesized by Sigma-Aldrich. The sequences of rat CREB antisense ODNs, 5′-TGGTCATCTAGTCACCGGTG-3′, and mmODN, 5′-GACCTCAGGTAGTCGTCGTT-3′ (synthesized by Sigma-Aldrich) were designed as reported previously (Ma et al., 2003). The rat C/EBPβ siRNA, 5′-CUGCUGGCCUCGGCGGGUC[dT][dT]-3′, and mismatch siRNA (mmRNA) 5′ GCGCGAUAGCGCGAAUAUA[dT][dT] 3′ were purchased, and both sequence were predesigned and validated by Sigma-Aldrich.

Data analysis. Behavioral data were analyzed by two-way ANOVA repeated-measure followed by Bonferroni test (GraphPad Prism; RRID:SCR_002798). The statistical significance of the differences of neurochemical changes was determined by the *t* test or one-way ANOVA *post hoc* test following Fisher's PLSD test (StatView5). All data were presented as mean ± SEM, and *p* values <0.05 were considered to be statistically significant.

Results

pC/EBPβ is involved in peripheral gp120-induced neuropathic pain in rats

In line with ours and others on well characterized model of HIV neuropathic pain (Herzberg and Sagen, 2001; Wallace et al., 2007a,b; Zheng et al., 2011), perineural HIV-1 gp120 induced a persistent lowered mechanical withdrawal threshold of the ipsilateral hindpaw as measured by von Frey filaments compared with contralateral paw and sham rats, $F_{(12,96),\ \text{interaction}} = 2.238, p < 0.05$; $F_{(4,96),\ \text{main effect time}} = 2.611$, $p < 0.05$; $F_{(3,24),\ \text{main effect treatment}} = 11.05$, $p < 0.0001$, two-way ANOVA repeated-measures (Fig. 1*A*). We also observed that there was a significant difference in mechanical threshold between ipsilateral and contralateral hindpaws in gp120 rats at days 7 ($p < 0.01$), 10 ($p < 0.01$), and 14 ($p < 0.001$; two-way ANOVA Bonferroni post-tests; Fig. 1*A*), which was similar to a

previous report (Wallace et al., 2007b). Mechanical threshold in ipsilateral hindpaws in gp120 rats was significantly lower than that in ipsilateral hindpaws in sham rats at day 7 ($p < 0.01$), 10 ($p < 0.01$), and 14 d ($p < 0.001$; two-way ANOVA Bonferroni post-tests; Fig. 1*A*). There was no significant difference in mechanical threshold between ipsilateral hindpaw and contralateral paws in sham rats (Fig. 1*A*).

Western blots showed that in sham rats there was no marked difference in the expression of pC/EBPβ between ipsilateral and contralateral SCDH in the SCDH 2 weeks post-gp120 (Fig. 1*B*), however, in gp120 rats pC/EBPβ in the ipsilateral SCDH was significantly higher than that in the contralateral SCDH ($p < 0.01$, *t* test; Fig. 1*C*). Similarly, in sham rats there was no significant difference in the expression of C/EBPβ between ipsilateral and contralateral SCDH at 2 weeks (Fig. 1*D*), however, in gp120 rats C/EBPβ in the ipsilateral SCDH was markedly higher than that in the contralateral SCDH ($p < 0.01$, *t* test; Fig. 1*E*). RT-qPCR assay showed that gp120 application increased the expression of mRNA of C/EBPβ in the SCDH 2 weeks post-gp120 compared with the sham group, $p < 0.001$, *t* test (Fig. 1*F*). Western blots showed that gp120 application evoked overexpression of pC/EBPβ in the ipsilateral SCDH compared with either naive or sham ipsilateral SCDH groups ($p < 0.05$ vs sham, $p < 0.01$ vs naive, one-way ANOVA, *post hoc* PLSD test, $n = 4$; Fig. 1*G*), indicating overexpression of pC/EBPβ in the ipsilateral SCDH in gp120 rats. There was no significant difference in pC/EBPβ of contralateral SCDH among naive, sham, or gp120 groups (data not shown). Expression of C/EBPβ in the ipsilateral SCDH in gp120 rats was markedly higher than that in the naive or sham group ($p < 0.001$ vs naive, $p < 0.001$ *vs* sham, one-way ANOVA, *post hoc* PLSD test, $n = 4$; Fig. 1*H*), revealing overexpression of C/EBPβ in the ipsilateral SCDH in gp120 rats; no significant difference in C/EBPβ of contralateral SCDH was seen among naive, sham, or gp120 groups (data not shown).

Low-magnification image showed pC/EBPβ immunostaining in the L4/5 lamina I–V of the SCDH (Fig. 1*I*). Double-immunostaining showed that 88.2 ± 1.5% of pC/EBP-IR-positive cells were colocalized with NeuN (a neuron marker; Fig. 1*J*), but ~5.3 ± 0.5% of pC/EBP-IR-positive cells seem overlaid with GFAP-IR (astrocytes marker; Fig. 1*K*) or ~4.2 ± 0.7% of pC/EBP-IR-positive cells with OX-42 (a microglia marker; Fig. 1*L*), suggesting that pC/EBPβ expression was mainly in the neuronal cells in the SCDH in gp120 rats.

To further verify the role of pC/EBPβ in the gp120 model, we knocked down C/EBPβ expression using intrathecal injection of C/EBPβ siRNA, and examined mechanical threshold. Twelve days after gp120 producing neuropathic pain, C/EBPβ siRNA or mmRNA was intrathecally administered once daily (5 μg) for 2 d. Intrathecal C/EBPβ siRNA significantly increased mechanical threshold; $F_{(5,50),\ \text{interaction}} = 8.59$, $p < 0.0001$; $F_{(5,50),\ \text{main effect time}} = 9.52$, $p < 0.0001$; $F_{(1,10),\ \text{main effect treatment}} = 7.96$, $p < 0.05$, two-way repeated-measures ANOVA (Fig. 1*M*). Mechanical withdrawal threshold in the C/EBPβ siRNA group was higher than that in mmRNA at day 1 and 2, $p < 0.001$ versus mmRNA, two-way ANOVA Bonferroni tests. Neither C/EBPβ siRNA nor mmRNA changed mechanical threshold in sham rats (data not shown). Western blots showed that there was a significant increase in pC/EBPβ expression in the ipsilateral SCDH in the gp120+mmRNA group compared with that in the sham+mmRNA group, $p < 0.01$, one-way ANOVA *post hoc* PLSD test (Fig. 1*N*). The pC/EBPβ expression in the gp120+C/EBPβ-siRNA group was lower than that in the gp120+mmRNA group, $p < 0.01$, one-way ANOVA *post hoc* PLSD test (Fig. 1*N*), suggesting C/EBPβ plays an important role in the gp120 neuropathic pain model.

Peripheral gp120 induced the expression of TNFα, TNFRI, and $mtO_2^{\cdot-}$ in the SCDH

We have reported that the perineural gp120 application increases mRNA of TNFα using quantitative real time RT-qPCR in the ipsilateral L4/5 SCDH (Zheng et al., 2011), and that TNFα immunoreactivity in the L4/5 spinal cord is overexpressed in the lamina I–V of the dorsal horn using immunohistochemistry assay (Zheng et al., 2011). Here using Western blots, we compared the expression of TNFα between ipsilateral and contralateral SCDH in both sham and gp120 rats at 2 weeks after gp120. We found that there was no significant difference in TNFα between ipsilateral and contralateral SCDH in sham animals (Fig. 2*A*), but TNFα in the ipsilateral SCDH of gp120 rats was higher than that in the contralateral SCDH, $p < 0.01$, *t* test (Fig. 2*B*). At 2 weeks post-gp120, peripheral gp120 increased TNFα at the ipsilateral SCDH compared with naive or sham ipsilateral SCDH; $p < 0.001$ versus naive or sham, one-way ANOVA, *post hoc* PLSD test, $n = 4$ (Fig. 2*C*), indicating the overexpression of TNFα at the ipsilateral SCDH in gp120 rats. No marked difference of TNFα at the contralateral SCDH was shown among naive, sham, or gp120 rats (data not shown). We also examined TNFRI expression in the SCDH. There was no significant difference in TNFRI between ipsilateral and contralateral SCDH in sham animals (Fig. 2*D*), but TNFRI in the ipsilateral SCDH of gp120 rats was higher than that in the contralateral SCDH at 2 weeks after gp120, $p < 0.001$, *t* test (Fig. 2*E*). HIV gp120 application increased TNFRI at the ipsilateral SCDH compared with naive or sham ipsilateral SCDH, $p < 0.001$ versus naive or sham, one-way ANOVA, *post hoc* PLSD test, $n = 4$ (Fig. 2*F*), revealing the overexpression of TNFRI at the ipsilateral SCDH in gp120 rats. No significant difference of TNFRI at the contralateral SCDH was observed among naive, sham, or gp120 rats (data not shown). The immunostaining revealed 100% of TNFRI-IR-positive cells were colocalized with NeuN (Fig. 2*G–I*), but not with glial markers GFAP or OX42 (data not shown).

ROS accumulation has been observed in the mitochondria of the SCDH neurons in a number of pain models (Schwartz et al., 2009; Kim et al., 2011; Salvemini et al., 2011; Kanao et al., 2015; Iida et al., 2016). mtROS interrelates with signaling events in the pathogenesis of chronic pain (Sui et al., 2013). To examine whether spinal ROS was involved in the gp120 pain model, we used MitoSox image to detect $mtO_2^{\cdot-}$ at the spinal L4–L5 segments as described in our recent work (Iida et al., 2016). The MitoSox-positive image in the sham and gp120 groups was shown in Figure 2, *J* and *K*. Almost all MitoSox signalling is colocalized with immunostaining of neuron marker NeuN, but not glial markers GFAP or OX42 (data not shown), indicating that mitochondrial superoxide was expressed in neurons, but not glia that was in line with our previous report (Kanda et al., 2016a). We observed that there was a significant increase in the number of MitoSox-positive cells in the gp120 group compared with that in the sham group in the ipsilateral spinal cord dorsal horn laminar I–II, III–V, and the total SCDH ($p < 0.01$, *t* test; Fig. 2*L*). There was a similar number of MitoSox-positive cells between ipsilateral and contralateral SCDH in sham rats, however, the number of MitoSox-positive cells in ipsilateral SCDH in gp120 rats was higher than that in the contralateral SCDH ($p < 0.001$, *t* test; Fig. 2*M*).

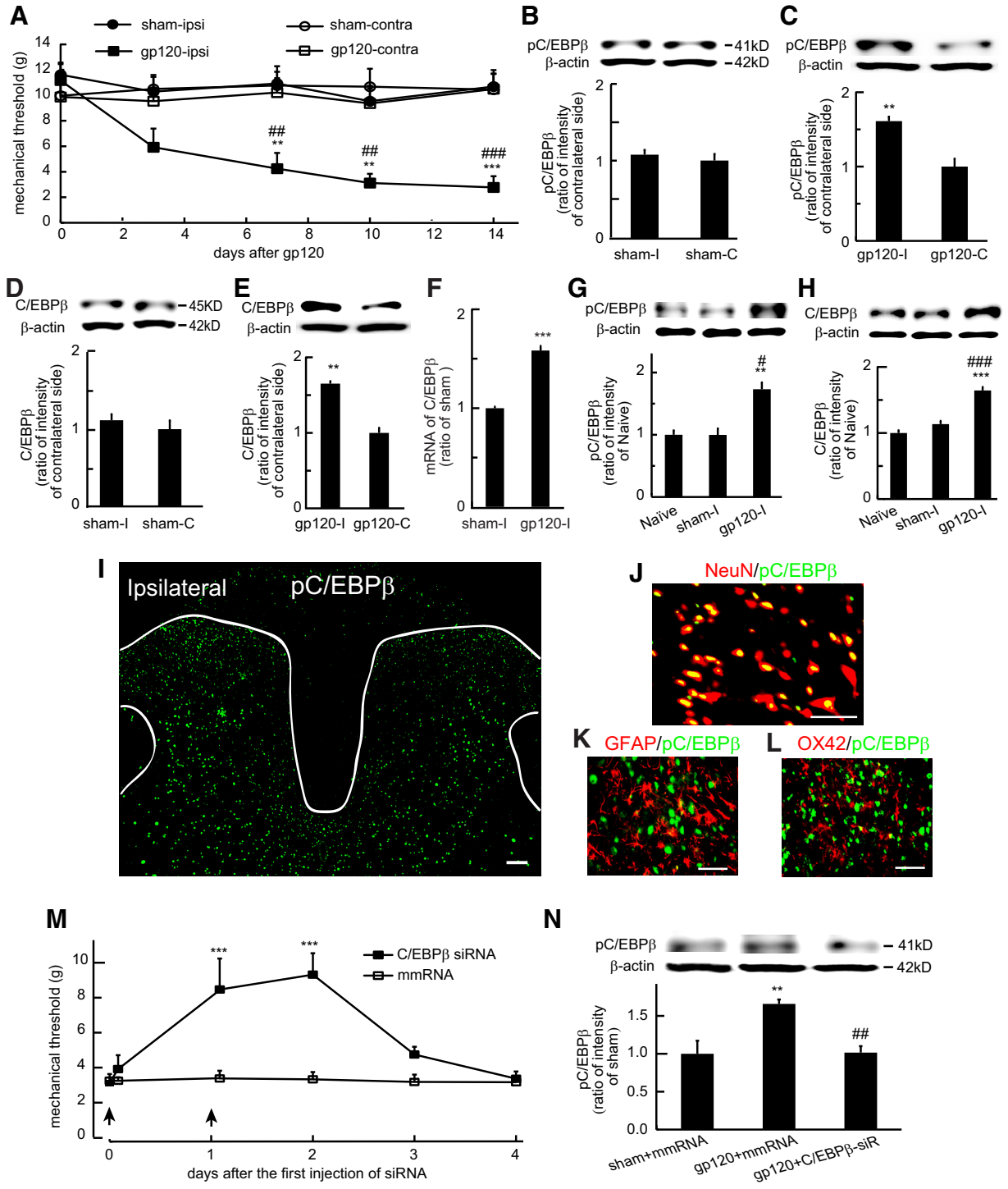

Figure 1. The expression of pC/EBPβ in the SCDH in the peripheral gp120 neuropathic pain model. ***A***, Rats received peripheral gp120 application onto the left sciatic nerve, and the sham group received RSA as vehicle. Time course of mechanical withdrawal threshold was measured using von Frey filaments to ipsilateral hindpaws and contralateral hindpaws. Peripheral gp120 induced a persistent lowered mechanical withdrawal threshold of the ipsilateral hindpaw as measured by von Frey filaments compared with sham rats; $F_{(12,96),\text{ interaction}} = 2.238, p < 0.05; F_{(4,96),\text{ main effect time}} = 2.611$, $p < 0.05; F_{(3,24),\text{ main effect treatment}} = 11.05, p < 0.0001$, two-way repeated-measures ANOVA; $n = 7$. We also observed that there was a significant lowered mechanical threshold in ipsilateral (gp120-ipsi) compared with that contralateral hindpaws (gp120-contra) in gp120 rats at days 7, 10, and 14 (**$p < 0.01$, ***$p < 0.001$ vs gp120-contralateral paw; two-way ANOVA, Bonferroni post-tests, $n = 7$. Mechanical threshold in ipsilateral hindpaws in gp120 rats (gp120-ipsi) was significantly lower than that in ipsilateral hindpaws in sham rats (sham-ipsi) at days 7, 10, and 14 (##$p < 0.01$, ###$p < 0.001$ vs sham-ipsilateral paw; two-way ANOVA, Bonferroni post-tests; $n = 7$. There was no significant difference in mechanical threshold between ipsilateral hindpaw (sham-ipsi) and contralateral paws (sham-contra) in sham rats. ***B***, Western blots showed no difference in the expression of pC/EBPβ in sham rats between ipsilateral (sham-I) and contralateral (sham-C) SCDH in the SCDH 2 weeks post-gp120. ***C***, pC/EBPβ in the ipsilateral SCDH in gp120 rats (gp120-I) was significantly higher than that in the contralateral SCDH (gp120-C); **$p < 0.01$, *t* test, $n = 6$. ***D***, No difference in the expression of C/EBPβ in sham rats between ipsilateral (sham-I) and contralateral SCDH (sham-C) at 2 weeks post vehicle. ***E***, C/EBPβ in the ipsilateral SCDH in gp120 rats (gp120-I) was significantly higher than that in the contralateral SCDH (gp120-C); **$p < 0.01$, *t* test, $n = 6$. ***F***, RT-PCR showed that gp120 increased the expression of mRNA of C/EBPβ; ***$p < 0.001$ versus sham, *t* test; $n = 5$. ***G***, Western blots assay showed that gp120 evoked overexpression of pC/EBPβ in the ipsilateral SCDH compared with either naive or sham groups; #$p < 0.05$ versus sham **$p < 0.01$ versus naïve; one-way ANOVA, *post hoc* PLSD test; $n = 4$. ***H***, HIV gp120 induced the overexpression of C/EBPβ in the ipsilateral SCDH; ***$p < 0.001$ versus naïve; ###$p < 0.001$ versus sham; one-way ANOVA, *post hoc* PLSD test; $n = 4$. ***I***, Low-magnification image showed pC/EBPβ immunostaining in the L4/5 lamina I–V of the SCDH. (*Figure legend continues.*)

Peripheral gp120 induced the expression of pCREB in the SCDH

Nociceptor afferents activation contributes to central sensitization through CREB-mediated transcriptional regulation in the SCDH neurons (Kawasaki et al., 2004). Previous studies demonstrated that pCREB plays an important role in neuropathic pain induced by nerve injury (Ma et al., 2003). Using Western blots we examined the expression of pCREB and CREB between ipsilateral and contralateral SCDH in both sham and gp120 rats at 2 weeks after gp120. There was no significant difference in pCREB (Fig. 3*A*) and CREB (Fig. 3*B*) between ipsilateral and contralateral SCDH in sham animals. However, pCREB in the ipsilateral SCDH of gp120 rats was higher than that in the contralateral SCDH ($p < 0.001$, *t* test; Fig. 3*C*). No significant change of CREB was shown in the ipsilateral and contralateral SCDH of gp120 rats (Fig. 3*D*). Expression of pCREB in ipsilateral SCDH in gp120 group was significantly higher than that in ipsilateral SCDH of naive or sham group ($p < 0.01$ vs naive or sham, one-way ANOVA, *post hoc* PLSD test, $n = 4$; Fig. 3*E*), indicating the overexpression of pCREB in the ipsilateral SCDH of gp120 rats. There was no significant difference in the expression of pCREB in contralateral SCDH among naive, sham, or gp120 groups (data not shown). There was no significant difference in total CREB in the ipsilateral SCDH 2 weeks post-gp120 compared with the sham group (Fig. 3*F*). Low-magnification image showed pCREB immunostaining in the SCDH (Fig. 3*G*). Double-immunostaining showed that 100% of pC/EBP-IR-positive cells were colocalized with NeuN (a neuron marker; Fig. 3*H*).

Peripheral gp120 increased pCREB bound on the C/EBPβ gene promoter region in the spinal cord dorsal horn

Previous studies suggest that pCREB induces C/EBPβ product through activating mRNA transcription of C/EBPβ (Pulido-Salgado et al., 2015). To determine whether pCREB activates C/EBPβ expression in the SCDH in an epigenetic manner, we used ChIP with quantitative PCR (ChIP-qPCR) assay in the gp120 neuropathic pain model. Two weeks after gp120, lumbar spinal cord dorsal ipsilateral to gp120 application were harvested for ChIP-qPCR. Figure 3*I* shows the alignment of rat C/EBPβ gene promoter regions (Pulido-Salgado et al., 2015) and qPCR primer area. We marked the two CRE binding locations and ChIP-qPCR primer areas before the transcriptional start site (TSS) of the C/EBPβ gene at rat chromosome 3 (ACCESSION #NC_005102.4; Fig. 3*I*). We found that gp120 application increased the enrichment of pCREB at the C/EBPβ gene promoter regions compared with sham ($p < 0.05$, *t* test; Fig. 3*J*). The results above suggested that CREB modulates the C/EBPβ gene expression in the transcriptional level.

Inhibition of TNFα signal blocked spinal $mtO_2^{\cdot-}$, pCREB, and pC/EBPβ in the gp120 pain model

We have reported that intrathecal administration of recombinant soluble TNF receptor I (rTNFSR), reversed the lowered mechanical threshold (reducing allodynia; Zheng et al., 2011). To determine whether TNFα-TNFRI signal initiated $mtO_2^{\cdot-}$, pCREB, and pC/EBPβ in the gp120 model, we intrathecally injected rTNFSR (50 ng; twice with 12 intervals to neutralize the bioactivity of TNFα) 2 weeks after gp120 application. MitoSox-positive images are shown in Figure 4*A–C* in the ipsilateral SCDH. The number of MitoSox-positive cells in the gp120+saline group was markedly more than that in the sham+saline group ($p < 0.01$, one-way ANOVA, *post hoc* PLSD test; Fig. 4*D*). There was a significant decrease in the MitoSox-positive cells in the gp120+rTNFSR group compared with that in the gp120+saline ($p < 0.01$, one-way ANOVA, *post hoc* PLSD test; Fig. 4*D*). Further, we examined the effect of intrathecal rTNFSR on the expression of pCREB and pC/EBPβ 2 weeks post-gp120 using Western blots. The expression of pCREB in ipsilateral SCDH in gp120+saline group was higher than that in sham+saline ($p < 0.01$, one-way ANOVA, *post hoc* PLSD test; Fig. 4*E*); there was a significant decrease in pCREB in gp120+rTNFSR compared with that in gp120+saline ($p < 0.05$, one-way ANOVA; Fig. 4*E*). Intrathecal rTNFSR did not change the expression of CREB (Fig. 4*F*). The expression of pC/EBPβ in the ipsilateral SCDH in gp120+saline group was higher than that in sham+saline ($p < 0.05$, one-way ANOVA, *post hoc* PLSD test; Fig. 4*G*); there was a significant decrease in pC/EBPβ in gp120+rTNFSR compared with that in gp120+saline ($p < 0.01$, one-way ANOVA; Fig. 4*G*). Western blots displayed that C/EBPβ in the gp120+saline group was higher than that in the sham+saline group ($p < 0.01$, one-way ANOVA; Fig. 4*H*); there was decrease in C/EBPβ in gp120+rTNFSR compared with that in gp120+saline ($p < 0.01$, one-way ANOVA; Fig. 4*H*). Also, TNFα in gp120+saline group was higher than that in sham+saline ($p < 0.01$, one-way ANOVA; Fig. 4*I*); TNFα in gp120+rTNFSR group was lower than that in gp120+saline ($p < 0.05$, one-way ANOVA; Fig. 4*I*). These results above suggested that spinal $mtO_2^{\cdot-}$, pCREB, and pC/EBPβ are downstream factors of TNFRI activity in the gp120-induced pain state.

The effect of knockdown of TNFRI on the $mtO_2^{\cdot-}$ pCREB, and pC/EBPβ in the gp120 model

To further determine the role of TNFRI in the gp120 model, we knocked down the TNFRI expression using antisense ODN against TNFRI (AS-TNFRI) in the gp120 model. We measured the anti-allodynic effect of intrathecal AS-TNFRI at the ipsilateral hindpaw. Ten days after gp120, AS-TNFRI or mmODN was intrathecally administered once daily (20 μg) for 5 d. Intrathecal AS-TNFRI increased mechanical threshold ($F_{(6,60),\ \text{interaction}} = 4.44$, $p < 0.001$; $F_{(6,66),\ \text{main effect time}} = 4.54$, $p < 0.001$; $F_{(1,10),\ \textit{main effect treatment}} = 16.09$; $p < 0.01$, two-way repeated-measures ANOVA, $n = 6$; Fig. 5*A*). Mechanical threshold in the group of AS-TNFRI group was higher than that in mismatch ODN at days 2–5 (two-way ANOVA, Bonferroni tests; Fig. 5*A*). Western blots displayed that gp120 increased TNFRI expression compared with sham (Fig. 5*B*), and that treatment with intrathecal AS-TNFRI reduced the upregulated TNFRI (Fig. 5*B*) at the ipsilateral SCDH (one-way ANOVA, PLSD test, $n = 4$) indicating that AS-TNFRI effectively knocked down the TNFRI protein expression.

To determine whether $mtO_2^{\cdot-}$, pCREB, and pC/EBPβ were downstream factors of TNFRI, we examined the effect of knockdown of TNFRI on $mtO_2^{\cdot-}$ in the ipsilateral SCDH. Five days after ODN, animals were perfused with 4% PFA 70 min after MitoSOx

←

(*Figure legend continued.*) Scale bar, 100 μm. ***J–L***, Double-immunostaining showed that pC/EBP-beta-positive cells were colocalized with NeuN (a neuron marker; ***J***), but few of pC/EBP-beta-positive cells overlaid with GFAP (astrocytes marker; ***K***) or with OX42 (a microglia marker; ***L***) in the SCDH in rats with gp120 application at 2 weeks. Scale bar, 50 μm. ***M***, Twelve days after gp120 application, intrathecal administration of C/EBPβ siRNA or mmRNA was given once a day for 2 d. Intrathecal C/EBPβ siRNA significantly increased mechanical threshold ($F_{(5,50),\ \text{interaction}} = 8.59$, $p < 0.0001$; $F_{(5,50),\ \text{main effect time}} = 9.52$, $p < 0.0001$; $F_{(1,10),\ \text{main effect treatment}} = 7.96$, $p < 0.05$; two-way repeated-measures ANOVA). Mechanical withdrawal threshold in the C/EBPβ siRNA group was higher than that in mmRNA at day 1 and 2; ***$p < 0.001$ versus mmRNA; two-way ANOVA, Bonferroni tests; $n = 6$. ***N***, Western blots displayed that C/EBPβ siRNA reversed the upregulated pC/EBPβ in the SCDH. **$p < 0.01$ versus sham+mmRNA; ##$p < 0.01$ versus gp120+mmRNA; one-way ANOVA, *post hoc* PLSD test; $n = 4–5$.

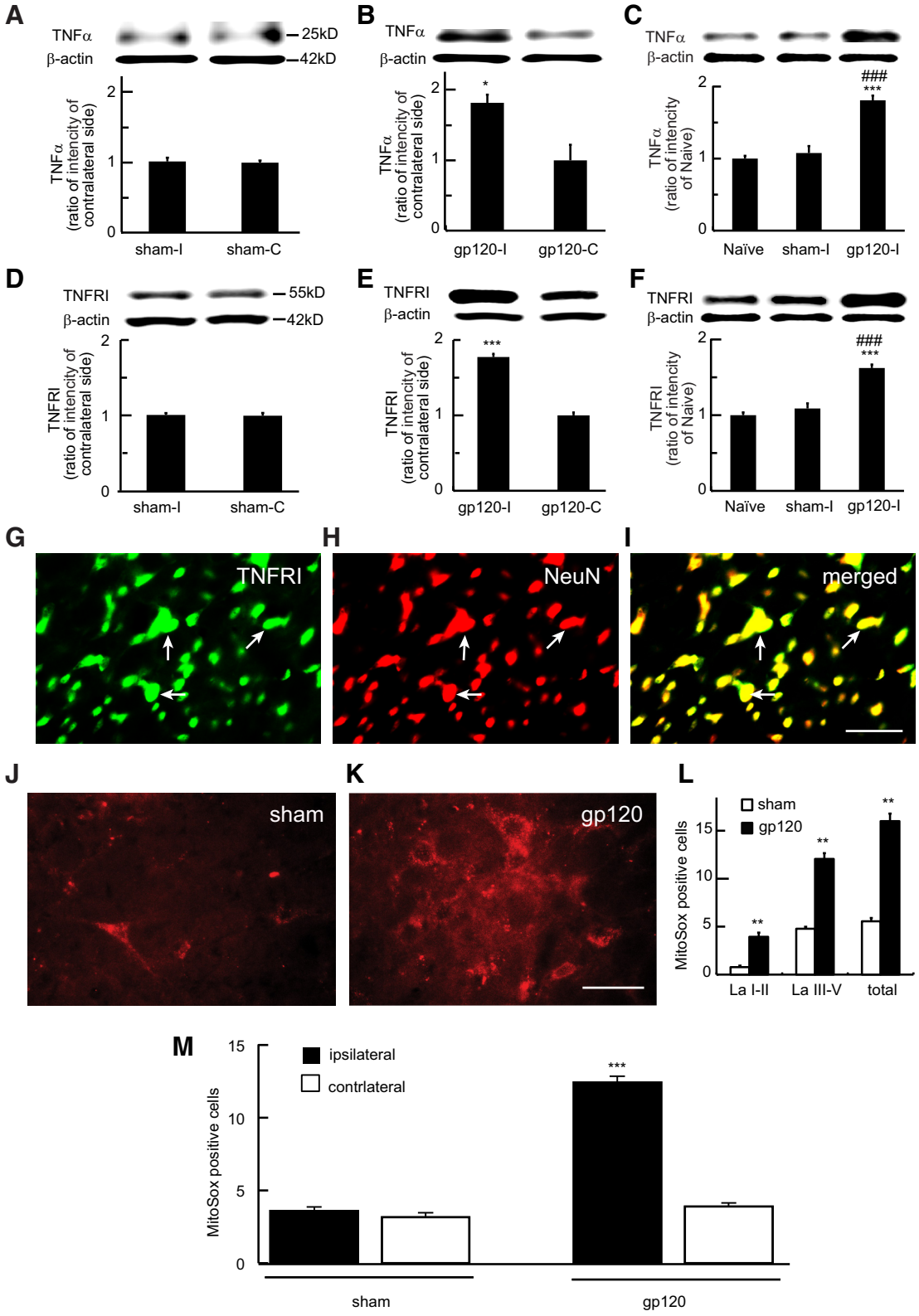

Figure 2. The increased expression of TNFα, TNFRI, and $mtO_2^{\cdot-}$ in the SCDH in the gp120 model. ***A–C***, The expression of TNFα between ipsilateral and contralateral SCDH in both sham and gp120 rats at 2 weeks after gp120, using Western blots. ***A***, No significant difference in TNFα between ipsilateral (sham-I) and contralateral (sham-C) SCDH in sham rats. ***B***, TNFα in the ipsilateral SCDH of gp120 rats (gp120-I) was higher than that in the contralateral SCDH (gp120-C); $^{*}p < 0.05$ versus gp120-C; *t* test, $n = 6$. ***C***, At 2 weeks after gp120, peripheral gp120 increased spinal TNFα at ipsilateral SCDH $^{***}p < 0.001$ versus Naive; $^{###}p < 0.001$ versus sham-I, one-way ANOVA, posthoc PLSD test. $n = 4$. ***D***, No significant difference in TNFRI between ipsilateral and contralateral SCDH in sham animals. ***E***, TNFRI in the ipsilateral SCDH of gp120 rats (gp120-I) was higher than that in the contralateral SCDH (gp120-C) at 2 weeks after gp120; $^{***}p < 0.001$, *t* test; $n = 6$. ***F***, HIV gp120 increased spinal TNFRI at ipsilateral SCDH (gp120-I) $^{***}p < 0.001$ versus Naive; $^{###}p < 0.001$ versus sham-I, one-way ANOVA, posthoc PLSD test; $n = 4$. ***G–I***, Double-immunostaining showed that TNFRI was colocalized with NeuN. Scale bar, 50 μm. ***J***, ***K***, Representative images of MitoSox-positive cells in the SCDH in rats with gp120 and sham surgery at 2 weeks. Scale bar, 50 μm. ***L***, HIV gp120 application increased MitoSox-positive cells in the lamina I–II, III–V, and total dorsal horn (laminar I–V) in the ipsilateral SCDH; $^{**}p < 0.01$, *t* test; $n = 5$. ***M***, The number of MitoSox-positive cells between ipsilateral and contralateral SCDH in sham rats, and in gp120 rats; $^{***}p < 0.001$, *t* test; $n = 4–5$.

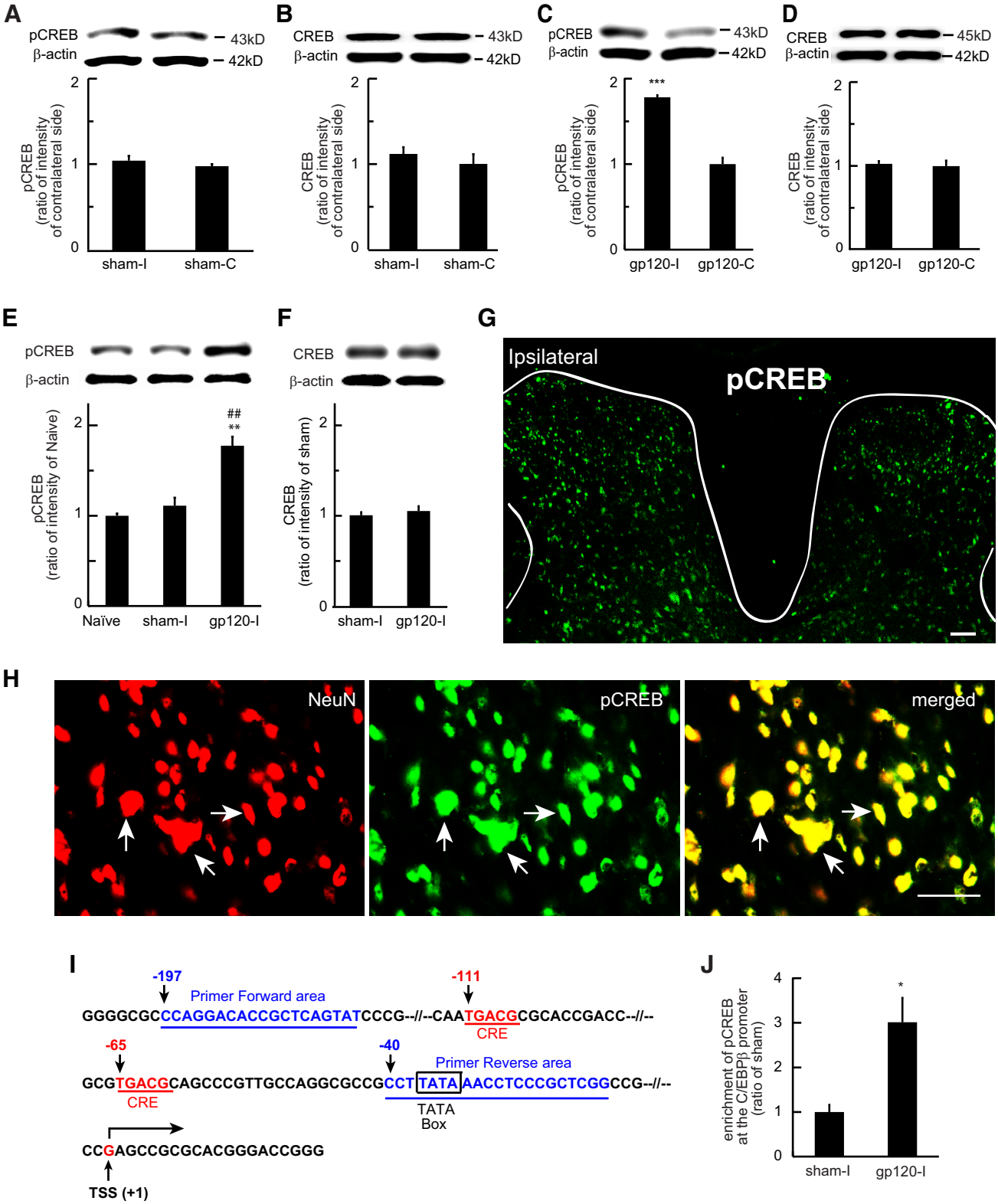

Figure 3. The expression of pCREB and its binding location at the C/EBPβ gene promoter regions in the peripheral gp120 neuropathic pain model. The expression of pCREB and CREB between ipsilateral and contralateral SCDH in both sham and gp120 rats at 2 weeks after gp120. No significant difference in pCREB (***A***) and CREB (***B***) between ipsilateral (sham-I) and contralateral SCDH (sham-C) in sham animals. ***C***, Expression of pCREB in the ipsilateral SCDH of gp120 rats (gp120-I) was higher than that in the contralateral SCDH (gp120-C); $^{***}p < 0.001$ versus gp120-C, *t* test; $n = 6$. ***D***, No significant change of CREB in the ipsilateral and contralateral SCDH of gp120 rats. ***E***, Western bolts showed that gp120 increased the expression of pCREB in the ipsilateral SCDH compared with naive or sham group; $^{**}p < 0.01$ versus naïve; $\#\#p < 0.01$ versus sham-I; one-way ANOVA, *post hoc* PLSD test; $n = 4$. ***F***, There was no significant difference between sham and gp120 group in CREB in the ipsilateral SCDH. ***G***, Low-magnification image showed pCREB immunostaining in the L4/5 lamina I–V of the SCDH. Scale bar, 100 μm. ***H***, Double-immunostaining showed that almost all of pCREB was colocalized with NeuN. Scale bar, 50 μm. ***I***, Alignment of rat *C/EBPβ* gene promoter regions, and pCREB binding location. We marked the CRE and ChIP-qPCR primer areas at the location before the TSS of the C/EBPβ gene at rat chromosome 3 (ACCESSION #NC_005102.4). ***J***, Application of gp120 increased the enrichment of pCREB at the C/EBPβ gene promoter regions in the ipsilateral SCDH compared with sham ipsilateral side; $^{*}p < 0.05$ versus sham-I, *t* test; $n = 5$.

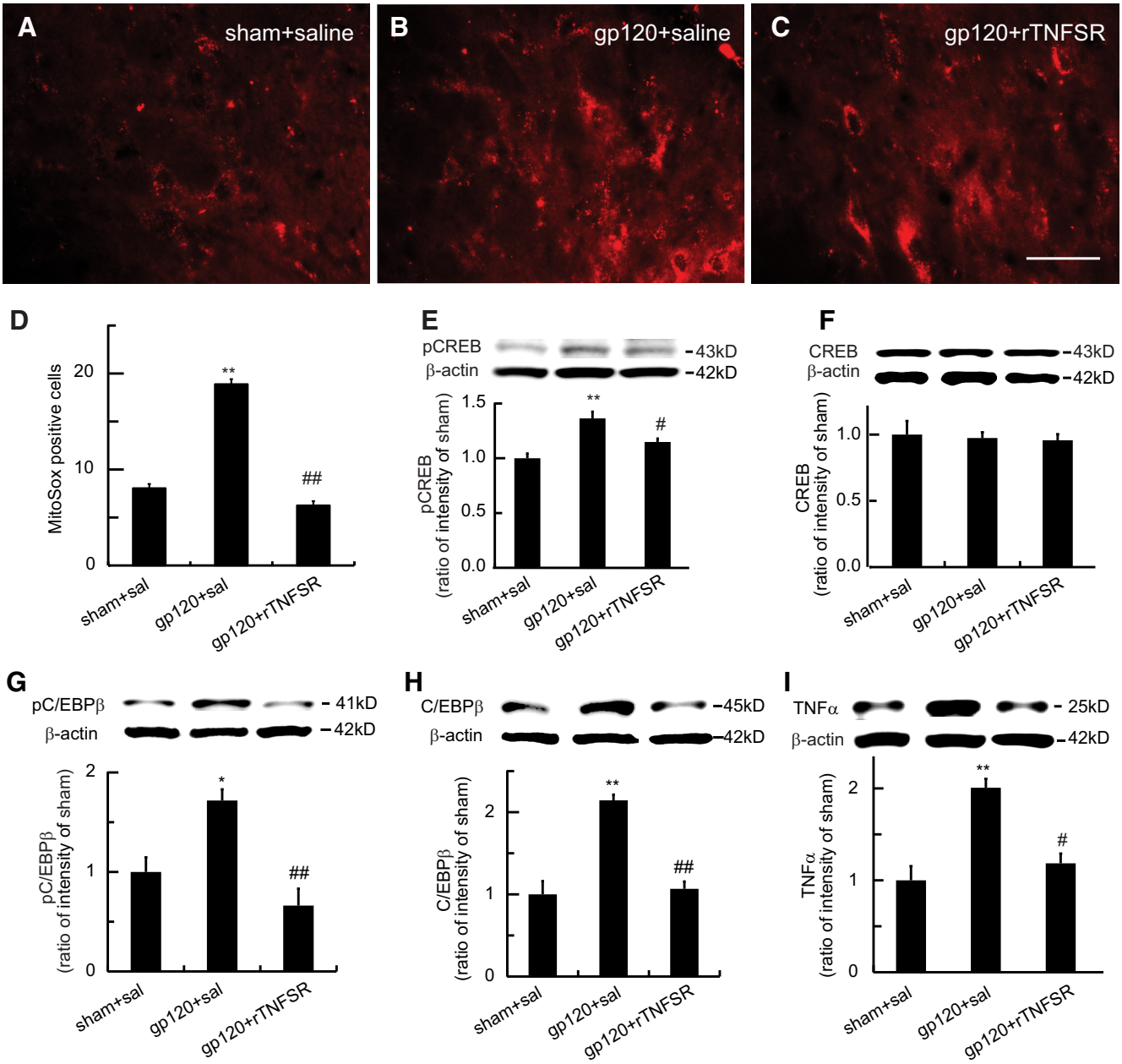

Figure 4. The effect of TNFα signal blockage with intrathecal rTNFSR on the expression of MitoSox cells, pCREB, and pC/EBPβ in the SCDH. ***A–C***, Representative MitoSox image in sham+saline (***A***), gp120+saline (***B***), and gp120+rTNFSR (***C***) was shown. Scale bar, 50 μm. ***D***, The number of MitoSox-positive cells in the ipsilateral SCDH was displayed; $^{**}p < 0.01$ versus the sham+saline group; $^{\#\#}p < 0.01$ versus gp120+saline group; one-way ANOVA, *post hoc* PLSD test; $n = 5–6$. ***E***, Western blots showed that the effect of intrathecal rTNFSR on pCREB in rats with gp120; $^{**}p < 0.01$ versus sham+saline; $^{\#}p < 0.05$ versus gp120+saline; one-way ANOVA, $n = 4$. ***F***, There was no significant change in the expression of CREB among groups of sham+saline, gp120+saline, and gp120+rTNFSR. ***G***, Effect of rTNFSR on pC/EBPβ in rats with gp120 using Western blots; $^{*}p < 0.05$ versus sham+saline; $^{\#\#}p < 0.01$ versus gp120+saline; one-way ANOVA; $n = 4–5$. ***H***, Effect of rTNFSR on C/EBPβ in rats with gp120 using Western blots; $^{**}p < 0.01$ versus sham+saline; $^{\#\#}p < 0.01$ versus gp120+saline; one-way ANOVA, $n = 4–5$. ***I***, The effect of rTNFSR on TNF_a in rats with gp120 using Western blots; $^{**}p < 0.01$ versus sham+saline; $^{\#}p < 0.05$ versus gp120+saline; one-way ANOVA, $n = 4–5$.

Red injection. MitoSox-positive image in groups of sham+mmODN, gp120+mmODN, or gp120+AS-TNFRI is shown in Figure 5*C*. The number of MitoSox-positive cells in the gp120+mmODN group was markedly more than that in the sham+mmODN group ($p < 0.001$, one-way ANOVA; $n = 4–5$; Fig. 5*D*). The number of MitoSox-positive cells in the gp120+AS-TNFRI group was lower than that in the gp120+mmODN group ($p < 0.001$, one-way ANOVA; Fig. 5*D*). Furthermore, Western blots displayed that knockdown of TNFRI using intrathecal AS-TNFRI, significantly lowered the upregulated pCREB in the SCDH (one-way ANOVA, $n = 4$; Fig. 5*E*), but AS-TNFRI or mmODN treatment did not markedly change CREB (Fig. 5*F*). Treatment with AS-TNFRI also suppressed the increased expression of pC/EBPβ (one-way ANOVA, $n = 4$; Fig. 5*G*) and C/EBPβ (one-way ANOVA, $n = 4$; Fig. 5*H*) in the SCDH. The results above indicate that TNFRI modulated downstream factors ($mtO_2^{\cdot-}$, pCREB, and pC/EBPβ) in the gp120 neuropathic pain model.

Intrathecal $mtO_2^{\cdot-}$ scavenger increased mechanical threshold and reduced pCREB and pC/EBPβ in the SCDH in the gp120 model

ROS as an important signaling molecule, regulates various cellular pathways (Brookheart et al., 2009). Superoxide is the main ROS produced by xanthine oxidase, the mitochondrial

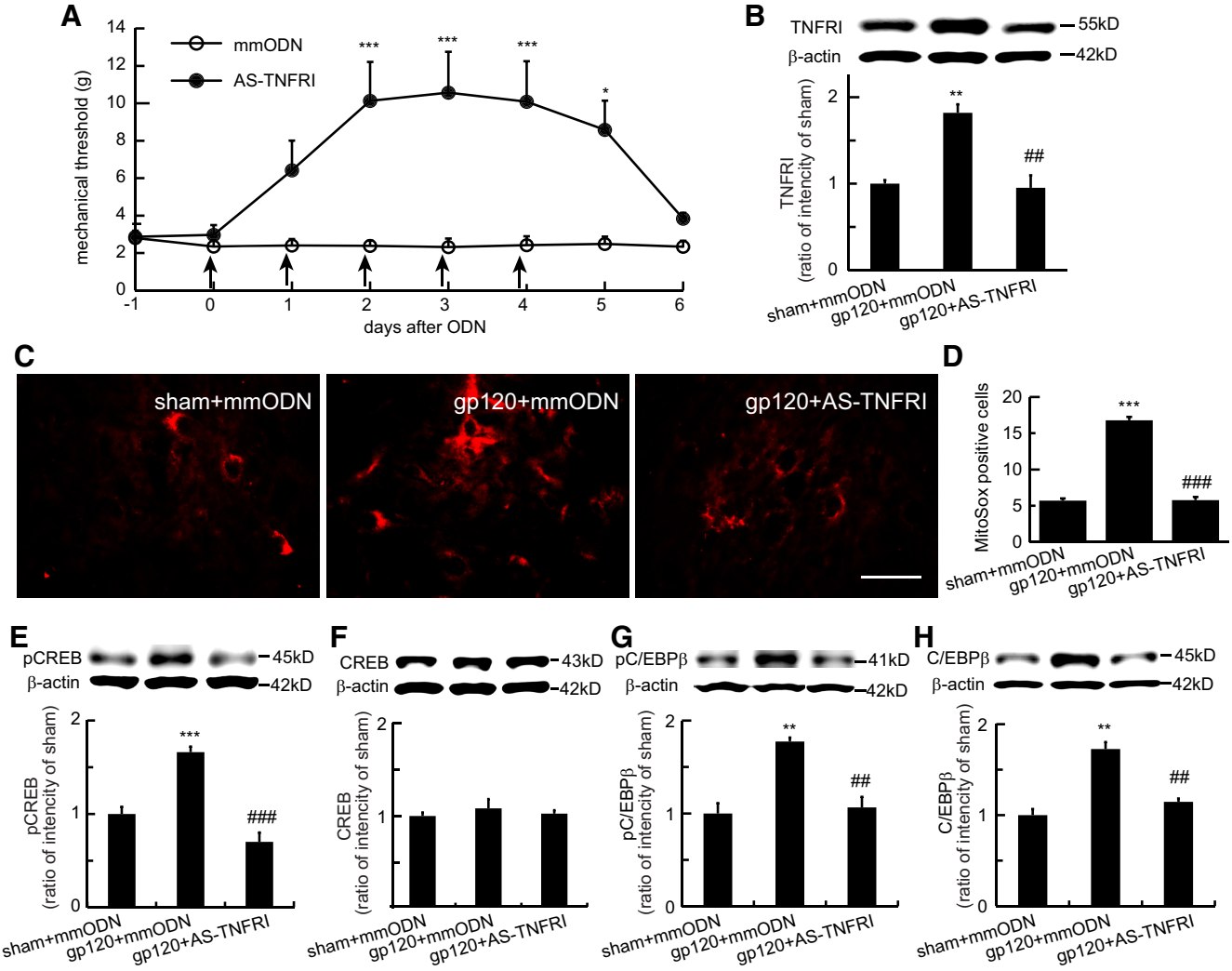

Figure 5. The effect of TNFRI knockdown on the expression of $mtO_2^{\cdot-}$, pCREB, and pC/EBPβ in the ipsilateral SCDH in the gp120 model. ***A***, Ten days after gp120, AS-TNFRI or mmODN was intrathecally administered once daily (20 μg) for 5 d. Intrathecal AS-TNFRI increased mechanical threshold; $F_{(6,60),\ \text{interaction}} = 4.44$, $p < 0.001$; $F_{(6,60),\ \text{main effect time}} = 4.54$, $p < 0.001$; $F_{(1,10),\ \textit{main effect treatment}} = 16.09$, $p < 0.01$; two-way repeated-measures ANOVA; $n = 6$. Mechanical threshold in the AS-TNFRI group was higher than that in mismatch ODN at days 2–5; $^{*}p < 0.05$; $^{***}p < 0.001$ versus mmODN; two-way ANOVA, Bonferroni tests. ***B***, HIV gp120 increased TNFRI expression compared with sham + mmODN; $^{**}p < 0.01$; one-way ANOVA, PLSD test, $n = 4$. TNFRI in gp120 + AS-TNFRI was lower than that in gp120 + mmODN; $\#\#p < 0.01$, one-way ANOVA, *post hoc* PLSD test; $n = 4$. ***C***, MitoSox-positive images in groups of sham + mmODN, gp120 + mmODN, or gp120 + AS-TNFRI are shown. ***D***, The number of MitoSox-positive cells in lamina I–V of ipsilateral SCDH in the sham + mmODN, gp120 + mmODN, and gp120 + AS-TNFRI groups; $^{***}p < 0.001$ versus sham + mmODN; $\#\#\#p < 0.001$ versus gp120 + mmODN; one-way ANOVA, *post hoc* PLSD test; $n = 4$–5. ***E***, Effect of knockdown of TNFRI on pCREB in the SCDH; $^{***}p < 0.001$ versus sham + mmODN; $\#\#\#p < 0.001$ versus gp120 + mmODN; one-way ANOVA, *post hoc* PLSD test; $n = 4$. ***F***, Effect of knockdown of TNFRI on CREB in the SCDH. ***G***, AS-TNFRI suppressed the increased expression of pC/EBP; $^{**}p < 0.01$ versus sham + mmODN; $\#\#p < 0.01$ versus gp120 + mmODN; one-way ANOVA, *post hoc* PLSD test; $n = 4$. ***H***, AS-TNFRI suppressed the increased expression of C/EBPβ; $^{**}p < 0.01$ versus sham + mmODN; $\#\#p < 0.01$ versus gp120 + mmODN; one-way ANOVA, *post hoc* PLSD test; $n = 4$.

respiratory chain, and nitric oxide enzymes. To investigate whether spinal $mtO_2^{\cdot-}$ played a role in neuropathic rats, we tested the anti-allodynic effect of new mitochondria-target superoxide scavenger Mito-T (50 μg). Intrathecal Mito-T significantly increased mechanical threshold compared with vehicle ($F_{(5,55),\ \text{interaction}} = 8.32$, $p < 0.0001$; $F_{(5,50),\ \text{main effect time}} = 7.80$, $p < 0.0001$; $F_{(1,11),\ \text{main effect treatment}} = 9.71$; $p < 0.01$, two-way repeated-measures ANOVA; Fig. 6*A*). Mechanical withdrawal threshold in the Mito-T group was higher than that in vehicle at 30–90 min ($p < 0.01$, two-way ANOVA, Bonferroni tests). Neither Mito-T nor vehicle changed mechanical threshold in the sham rats (data not shown). To examine whether there was a relationship between $mtO_2^{\cdot-}$ and pCREB or pC/EBPβ in the gp120 model, 2 weeks post-gp120, intrathecal Mito-T was administered. One hour after Mito-T, the ipsilateral SCDH was harvested for Western blot analysis. There was a significant increase in the expression of pCREB in gp120+saline group compared with that in sham+saline ($p < 0.05$, one-way ANOVA; Fig. 6*B*); pCREB in gp120+Mito-T group was lower than that in gp120+saline ($p < 0.01$, one-way ANOVA; Fig. 6*B*). Similarly, there was a markedly increase in the expression of pC/EBPβ in gp120+saline group compared with that in sham+saline ($p < 0.01$, one-way ANOVA; Fig. 6*C*); pC/EBPβ in gp120+Mito-T group was lower than that in gp120+saline ($p < 0.01$, one-way ANOVA; Fig. 6*C*), suggesting that spinal pCREB and pC/EBPβ are downstream factors of $mtO_2^{\cdot-}$.

Knockdown of spinal CREB increased mechanical threshold and reduced pC/EBPβ in the gp120 neuropathic pain model

To examine whether CREB is involved in the gp120 neuropathic pain model, we knocked down CREB expression using intrathecal antisense ODN against the nuclear transcription factor CREB

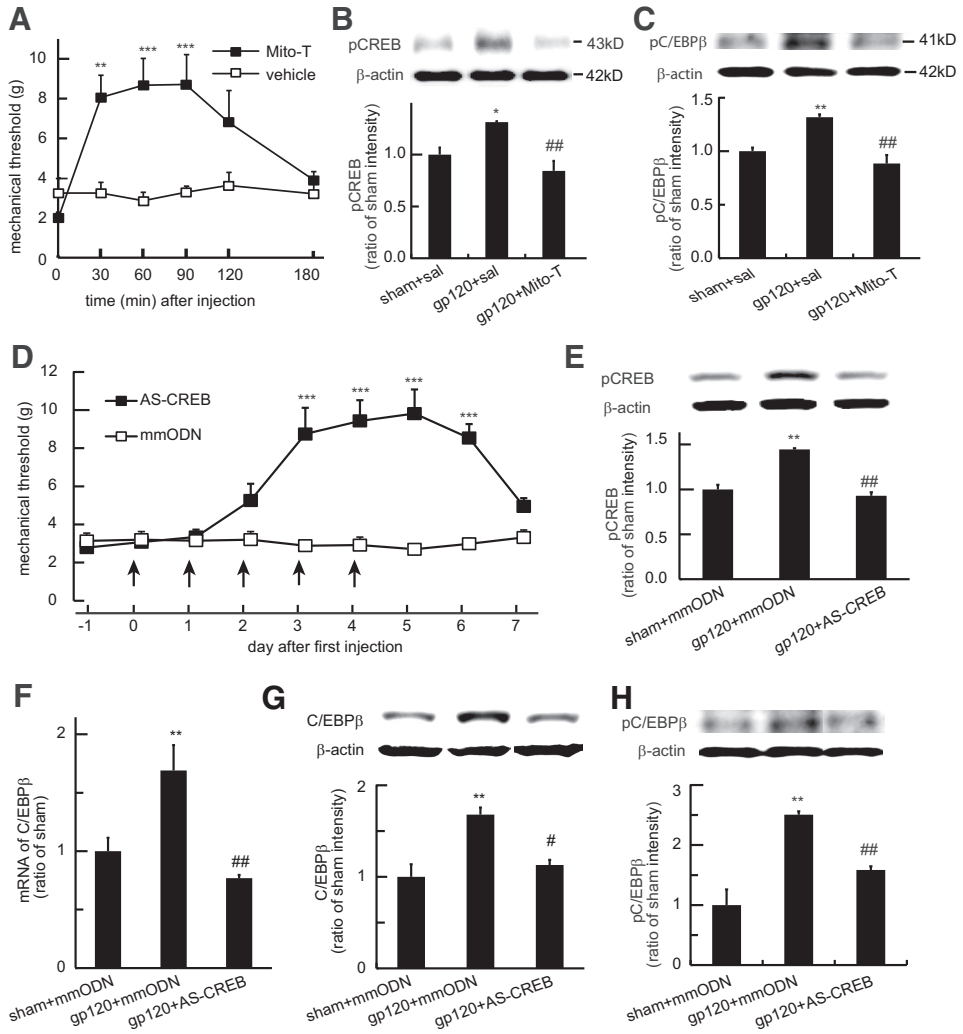

Figure 6. The effect of inhibition of $mtO_2^{\cdot-}$ signal and the knockdown of CREB on the gp120 neuropathic pain. ***A***, HIV gp120 neuropathic rats received intrathecal Mito-Tempol (Mito-T, 50 μg) or saline (vehicle). Mito-T significantly increased mechanical threshold compared with vehicle; $F_{(5,55),\text{ interaction}} = 8.32, p < 0.0001; F_{(5,50),\text{ main effect time}} = 7.80, p < 0.0001; F_{(1,11),\text{ main effect treatment}} = 9.71$, $p < 0.01$; two-way repeated-measures ANOVA. Mechanical withdrawal threshold in the Mito-T group was higher than that in vehicle at 30–90 min; $^{**}p < 0.01$, $^{***}p < 0.001$, two-way repeated-measures ANOVA with Bonferroni test; $n = 6$–7. ***B***, The effect of Mito-Tempol on pCREB in the ipsilateral SCDH using Western blots; $^{*}p < 0.05$ versus sham+saline group; $^{\#\#}p < 0.01$ versus gp120+saline group; one-way ANOVA, *post hoc* PLSD test; $n = 4$. ***C***, The effect of Mito-Tempol on pC/EBPβ in the gp120 model using Western blots; $^{**}p < 0.01$ versus sham+saline group; $^{\#\#}p < 0.01$ versus gp120+saline group; one-way ANOVA, *post hoc* PLSD test; $n = 4$. ***D***, The effect of the knockdown of CREB using antisense ODN against CREB on mechanical threshold in the gp120 model. Intrathecal AS-CREB significantly increased mechanical threshold; $F_{(8,88),\text{ interaction}} = 8.86, p < 0.0001; F_{(8,88),\text{ main effect time}} = 7.00, p < 0.0001; F_{(1,11),\text{ main effect treatment}} = 30.04, p < 0.001$; two-way repeated-measures ANOVA; $n = 6$–7. Mechanical withdrawal threshold in the antisense ODN of CREB group was higher than that in mismatch ODN at days 3–6; $^{***}p < 0.001$, two-way repeated-measures ANOVA with Bonferroni test; $n = 6$–7. ***E***, The effect of AS-CREB on the expression of pCREB in the ipsilateral SCDH; $^{**}p < 0.01$ versus sham+mmODN group; $^{\#\#}p < 0.01$ versus gp120+mmODN group; one-way ANOVA, *post hoc* PLSD test; $n = 4$. ***F–H***, Knockdown of spinal CREB on the C/EBPβ mRNA, C/EBPβ, or pC/EBPβ in the ipsilateral SCDH of gp120 neuropathic rats. Intrathecal AS-CREB (once a day for 5 d) reversed the upregulation of C/EBPβ mRNA using RT-PCR (***F***) and C/EBPβ protein using Western blots (***G***); $^{**}p < 0.01$ versus sham+mmODN group; $^{\#}p < 0.05$, $^{\#\#}p < 0.01$ versus gp120+mmODN group; one-way ANOVA, $n = 4$. Similarly, intrathecal AS-CREB reversed the upregulation of pC/EBPβ using Western blots (***H***); $^{**}p < 0.01$ versus sham+mmODN group; $^{\#\#}p < 0.01$, versus gp120+mmODN group; one-way ANOVA, $n = 4$.

mRNA. Ten days after gp120, AS-CREB or mmODN was intrathecally administered once daily (20 μg) for 5 d as described previously (Ma et al., 2003; Ferrari et al., 2015a). Intrathecal AS-CREB significantly increased mechanical threshold ($F_{(8,88),\text{ interaction}} = 8.86$, $p < 0.0001$; $F_{(8,88),\text{ main effect time}} = 7.00$, $p < 0.0001$; $F_{(1,11),\text{ main effect treatment}} = 30.04$; $p < 0.001$, two-way repeated-measures ANOVA; $n = 6$–7; Fig. 6*D*). Mechanical withdrawal threshold in the group of antisense ODN against CREB was higher than that in mismatch ODN at day 3–6 (two-way ANOVA, Bonferroni tests; Fig. 6*D*). To examine neurochemical changes, we harvested the ipsilateral SCDH at 2 h after the last injection of ODN. Western blots showed there was a significant increase in the expression of pCREB in gp120+mmODN group compared with that in sham+saline ($p < 0.01$, one-way ANOVA; Fig. 6*E*); pCREB in gp120+AS-CREB group was lower than that in gp120+mmODN ($p < 0.01$, one-way ANOVA; Fig. 6*E*). Meanwhile, knockdown of spinal CREB reversed the upregulation of C/EBPβ mRNA using RT-PCR (Fig. 6*F*) and C/EBPβ protein using Western blots (Fig. 6*G*). Similarly, knockdown of spinal CREB reversed the upregulation of pC/EBPβ using Western blots (Fig. 6*H*), suggesting that spinal C/EBPβ is a downstream factor of CREB in the neuropathic pain model.

Intrathecal MitoSox injection did not change expression of pCREB and pC/EBPβ in the SCDH in naive rats

To define whether MitoSox injection induces spinal pCREB and pC/EBPβ in the SCDH, we intrathecally administered MitoSox (33 μM, 30 μl) in naive rats. Saline was injected in vehicle group. Seventy

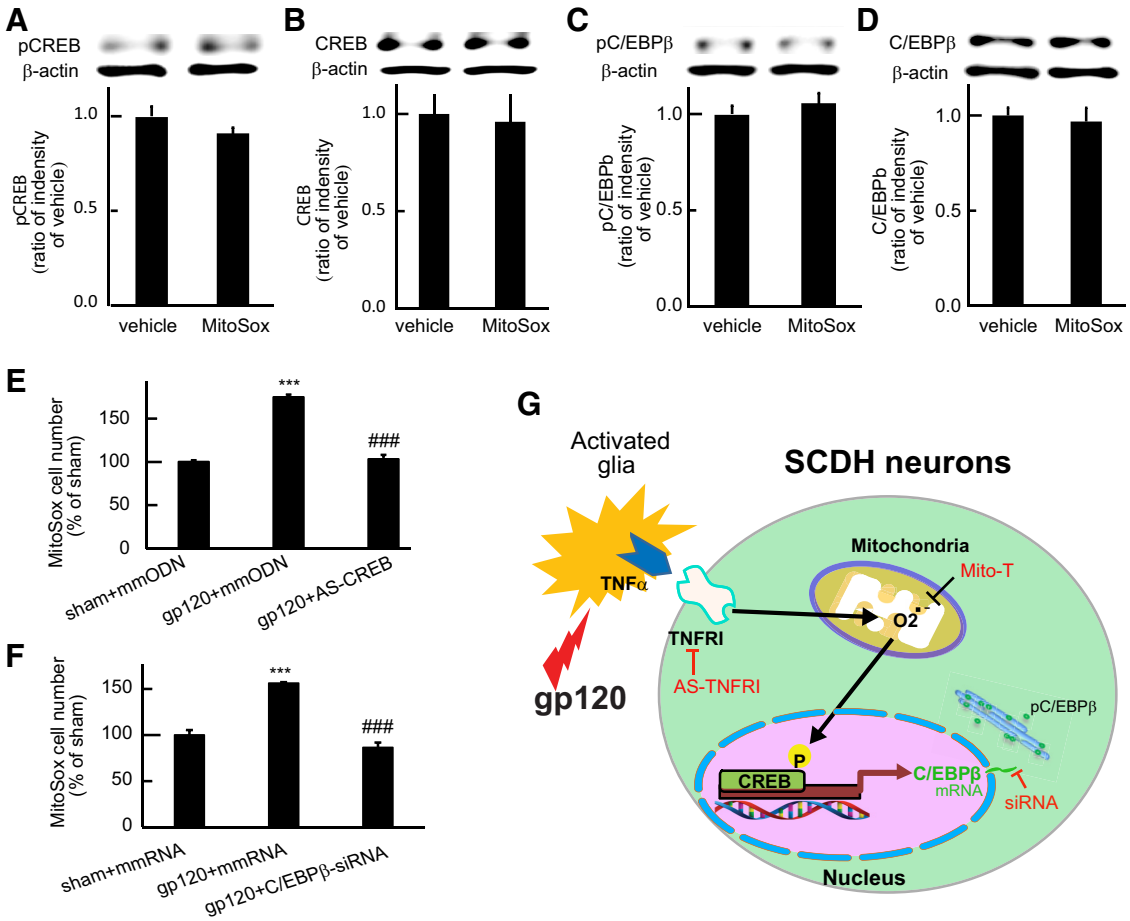

Figure 7. The effect of intrathecal MitoSox on pCREB, pC/EBPβ or C/EBPβ in naive rats, and the effect of the knockdown of CREB and C/EBPβ on $mtO_2^{\cdot-}$ in the gp120 neuropathic pain rats. ***A–D***, Seventy minutes after rats received intrathecal MitoSox or vehicle injection, the SCDH was harvested. Western blots showed that there was no significant difference in the expression of pCREB (***A***), CREB (***B***), pC/EBPβ (***C***), or C/EBPβ (***D***) in the SCDH 70 min after MitoSox compared with vehicle. ***E***, Effect of knockdown of spinal CREB on mitochondrial superoxide in the gp120 pain model. Ten days after gp120, AS-CREB or mmODN was intrathecally administered once daily (20 μg) for 5 d. One hour after the last ODN, MitoSox was intrathecally injected. Animals were perfused 70 min after MitoSox, and the spinal cord was harvested for MitoSox imagine. There was a significant increase in MitoSox-positive cells in gp120+mmODN group compared with that in sham+mmODN. ***$p < 0.001$, one-way ANOVA; $n = 5$. MitoSox-positive cells in gp120+AS-CREB group was lower than that in gp120+mmODN. ###$p < 0.001$, one-way ANOVA; $n = 5$. ***F***, Effect of knockdown of spinal C/EBPβ on mitochondrial superoxide in the gp120 pain model. Ten days after gp120, C/EBPβ siRNA or mmRNA was intrathecally administered once daily for 2 d. One hour after the last C/EBPβ siRNA or mmRNA, MitoSox was intrathecally injected. Animals were perfused 70 min after MitoSox, and the spinal cord was harvested for MitoSox imagine. There was a significant increase in MitoSox-positive cells in gp120+mmRNA group compared with that in sham+mmRNA. ***$p < 0.001$, one-way ANOVA; $n = 5$. MitoSox-positive cells in gp120+C/EBPβ siRNA group was lower than that in gp120+mmRNA. ###$p < 0.001$, one-way ANOVA; $n = 5$. ***G***, The proposed signaling pathways that TNFα–$mtO_2^{\cdot-}$–pCREB signaling pathway triggered the pC/EBPβ in gp120-related neuropathic pain in the spinal cord dorsal horn. HIV gp120 induced glia activity to release spinal TNFα (Zheng et al., 2011). TNFα binds its receptor TNFRI on the neurons. TNFRI signal increases mitochondrial ROS through unknown factors. ROS can lead to the activation of various other cell signaling pathway components, for example, transcriptional factor pCREB. pCREB may induce C/EBP expression (for review, see Alberini, 2009). C/EBPβ promotes recycling of NMDA receptors from endosomes to the plasma membrane (Wang et al., 2013). NMDA receptors increase Ca^{2+} influx (Ohno et al., 2002; Valnegri et al., 2015). Mitochondria are the major sites of ROS production in neurons, and participate in the regulation of cellular Ca^{2+} homeostasis, which is implicated in mitochondrial ROS generation (Camello-Almaraz et al., 2006; Kann and Kovacs, 2007; Douda et al., 2015). Thus, based on our results and previous evidence, we think that it is possible that pathway of TNFα/TNFRI signal triggering ROS–pCREB–pC/EBP through unknown pathways, is involved in the gp120 neuropathic pain state.

minutes after intrathecal of MitoSox or saline, the spinal cord was harvested for Western blot assay. There was no significant difference in the expression of pCREB (Fig. 7*A*), CREB (Fig. 7*B*), pC/EBPβ (Fig. 7*C*), or C/EBPβ (Fig. 7*D*) between vehicle and MitoSox.

Knockdown of CREB or C/EBPβ reduced spinal $mtO_2^{\cdot-}$ in the gp120 neuropathic pain model

As transcriptional factors, CREB or C/EBPβ may hold many functions to regulate neuropathic pain. C/EBPβ regulates sorting nexin 27 (SNX27; regulating endocytic sorting and trafficking), which promotes recycling of NMDA receptors from endosomes to the plasma membrane (Wang et al., 2013). NMDA receptors increase Ca^{2+} influx (Ohno et al., 2002; Valnegri et al., 2015). There is an interaction of cytosolic Ca^{2+} and mitochondrial ROS generation (Kann and Kovács, 2007; Korbecki et al., 2013; Douda et al., 2015). It is possible that CREB or C/EBPβ may affect spinal ROS. To examine the effect of CREB on spinal $mtO_2^{\cdot-}$ in the gp120 neuropathic pain model, we knocked down the CREB expression using intrathecal ODN antisense against CREB mRNA. Ten days after gp120, AS-CREB, or mmODN was intrathecally administered (once daily 20 μg for 5 d). One hour after the last ODN, MitoSox was intrathecally injected. Animals were perfused 70 min after MitoSox, and the spinal cord harvested for MitoSox imagines. There was a significant increase in MitoSox-positive cells at the ipsilateral SCDH in gp120+mmODN group compared with that in sham+mmODN ($p < 0.001$, one-way ANOVA; Fig. 7*E*); MitoSox-positive cells in gp120+AS-CREB group was lower than that in gp120+mmODN ($p < 0.001$, one-way ANOVA; Fig. 7*E*).

To examine whether C/EBPβ affects spinal $mtO_2^{\cdot-}$ in the gp120 neuropathic pain model, we knocked down the C/EBPβ expression

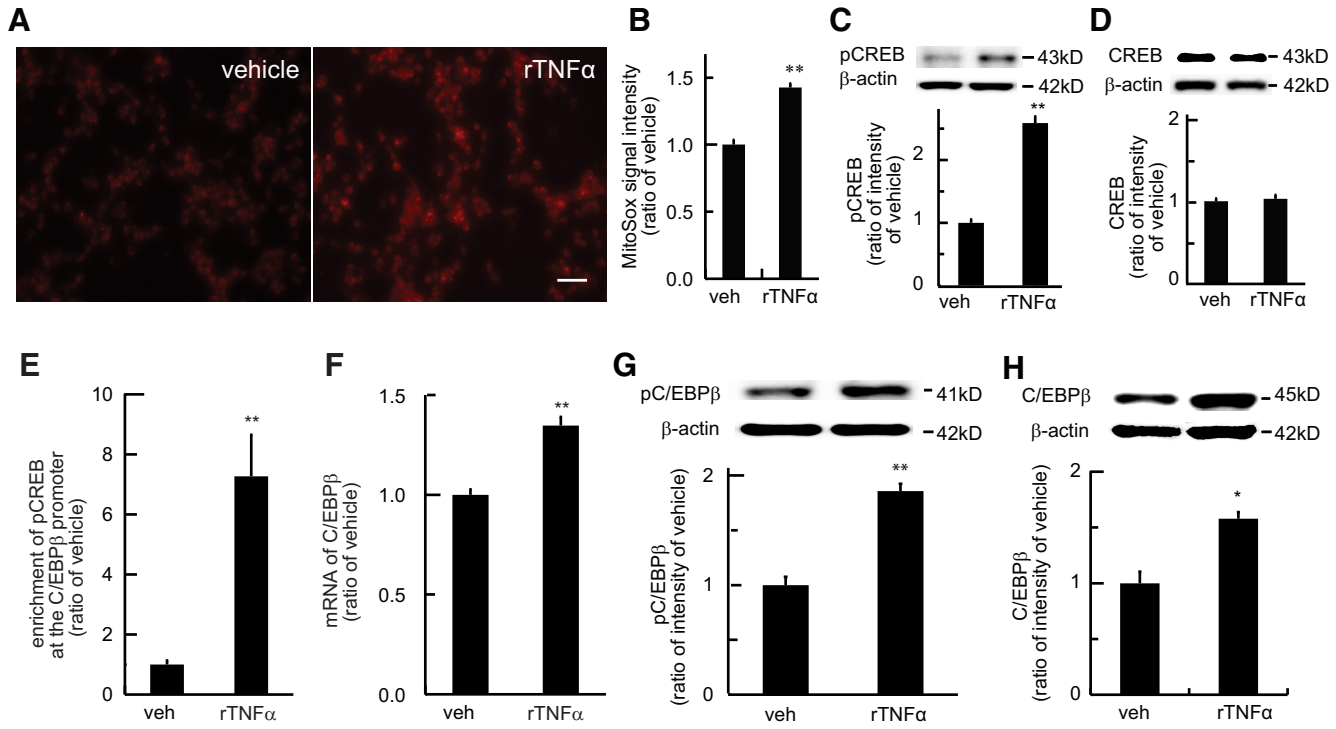

Figure 8. Recombinant TNFα induced mitochondrial superoxide, pCREB, and pC/EBPβ in the cultured B35 neuronal cell line. ***A***, Representative image of MitoSox for $mtO_2^{\cdot-}$ in the cultured neuronal cells. Scale bar, 50 μm. ***B***, The treatment with rTNFα significantly increased MitoSox signals in the B35 neuronal cells compared with vehicle treatment. $^{**}p < 0.01$, *t* test; $n = 3$. ***C***, The treatment with rTNFα increased pCREB compared with that with vehicle ($^{**}p < 0.01$, *t* test; $n = 3$–4), but not total CREB protein (***D***). ***E***, ChIP assay showed that treatment with rTNFα increased the binding of pCREB on the C/EBPβ promoter region; $^{**}p < 0.01$ versus vehicle; *t* test, $n = 3$. ***F***, Treatment with rTNFα increased the expression of C/EBPβ mRNA in the cultured B35 cells; $^{**}p < 0.01$ versus vehicle; *t* test, $n = 3$. ***G***, The treatment with rTNFα in the B35 cells increased pC/EBPβ protein expression compared with vehicle. $^{**}p < 0.01$, *t* test. ***H***, C/EBPβ protein was increased by rTNFα in the cultured neurons. $^{*}p < 0.05$, *t* test; $n = 3$.

using intrathecal C/EBPβ siRNA. Ten days after gp120, C/EBPβ siRNA or mmRNA was intrathecally administered once daily (5 μg/d) for 2 d. One hour after the last C/EBPβ siRNA or mmRNA, MitoSox was intrathecally injected. Animals were perfused 70 min after MitoSox, and the spinal cord was harvested for MitoSox imagine. There was a significant increase in MitoSox-positive cells at the ipsilateral SCDH in gp120+mmRNA group compared with that in sham+mmRNA ($p < 0.001$, one-way ANOVA; Fig. 7*F*); MitoSox-positive cells in gp120+ C/EBPβ siRNA group was lower than that in gp120+mmRNA ($p < 0.001$, one-way ANOVA; Fig. 7*F*), suggesting that pCREB or pC/EBPβ mediates the mitochondrial superoxide through unknown mechanisms in the HIV neuropathic pain model (Fig. 7*G*).

Recombinant TNFα induced $mtO_2^{\cdot-}$, pCREB, and pC/EBPβ in the cultured neurons *in vitro*

To further verify that pC/EBPβ was triggered by TNFα–$mtO_2^{\cdot-}$–pCREB pathway, we used rat neuronal B35 cells treated with rTNFα for 3 h for neurochemical analysis. Live cells were stained with MitoSox for 30 min at 37°C (Ahmed et al., 2012). The image of MitoSox in the cultured cells was shown in Figure 8*A*. The treatment with rTNFα increased the MitoSox signal compared with saline (vehicle; $p < 0.01$, *t* test, $n = 3$; Fig. 8*B*). The expression of pCREB in B35 cells treated with rTNFα was increased compared with that with vehicle, $p < 0.01$, *t* test (Fig. 8*C*), but the treatment with rTNFα in the B35 cells did not increase CREB protein expression compared with vehicle (Fig. 8*D*). ChIP-qPCR assay showed that treatment with rTNFα significantly increased the binding of pCREB on the C/EBPβ promoter region ($p < 0.01$, *t* test, $n = 3$; Fig. 8*E*). RT-qPCR displayed that rTNFα markedly increased C/EBPβ mRNA in the cultured B35 cells ($p < 0.01$, *t* test, $n = 5$; Fig. 8*F*). The treatment with rTNFα in the B35 cells increased pC/EBPβ protein expression compared with vehicle ($p < 0.01$, *t* test; Fig. 8*G*). Also, rTNFα increased C/EBPβ protein compared with vehicle ($p < 0.05$, *t* test; Fig. 8*H*). Thus, in the cultured neurons, rTNFα induced the upregulation of $mtO_2^{\cdot-}$, and increased pCREB and pC/EBPβ.

Relationship among TNFα, $mtO_2^{\cdot-}$, pCREB, and pC/EBPβ in the B35 cells treated with rTNFα

To further define the relationship among TNFα, $mtO_2^{\cdot-}$, pCREB, or pC/EBPβ, we treated neuronal B35 cells with Mito-T under the rTNFα application. MitoSox-positive imaging is shown in Figure 9*Aa*–*Ac*. The MitoSox signal density in the rTNFα+vehicle group was higher than that in the vehicle+vehicle, $p < 0.001$, one-way ANOVA, *post hoc* PLSD test (Fig. 9*B*). There was a significant decrease in the MitoSox signal density in the rTNFα+Mito-T group compared with that in rTNFα+vehicle ($p < 0.001$, one-way ANOVA *post hoc* PLSD test; Fig. 9*B*). Western blot analysis displayed that the expression of pCREB in the rTNFα+vehicle group was higher than that in the vehicle+vehicle ($p < 0.001$, one-way ANOVA, *post hoc* PLSD test; Fig. 9*C*). There was a significant decrease in pCREB in the rTNFα+Mito-T group compared with that in rTNFα+vehicle ($p < 0.001$, one-way ANOVA *post hoc* PLSD test; Fig. 9*C*). Similarly, Mito-T blocked the upregulated pC/EBPβ (Fig. 9*D*) and C/EBPβ (Fig. 9*E*), suggesting that increased pCREB or pC/EBPβ was in an $mtO_2^{\cdot-}$-dependent manner in the cultured B35 cells treated by rTNFα.

To confirm CREB mediating pC/EBPβ in the B35 cells treated with rTNFα, we gave antisense ODN against CREB to the B35

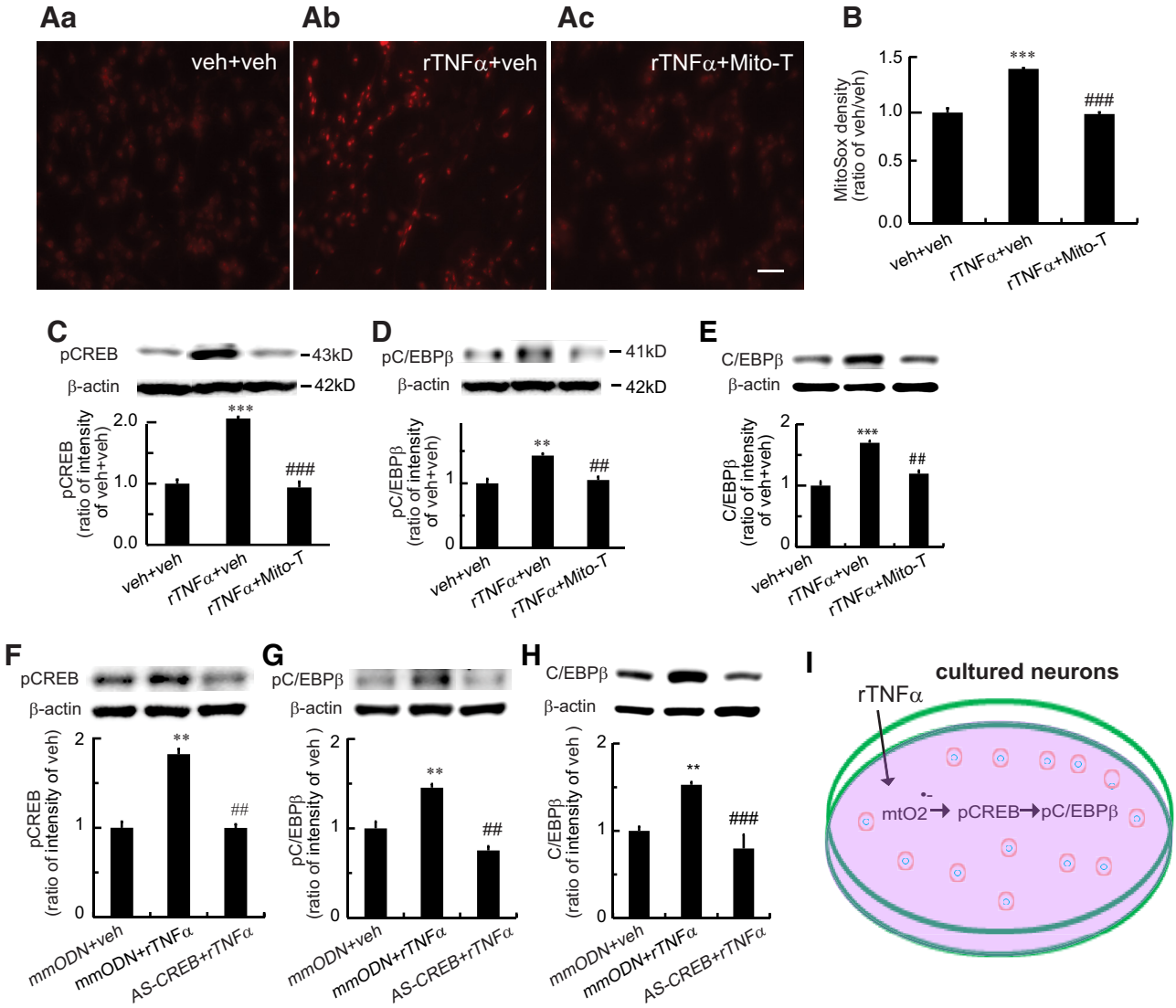

Figure 9. The relationship among $mtO_2^{\cdot-}$, pCREB, and pC/EBPβ in the cultured B35 neuronal cells treated with rTNFα. ***A***, Representative imaging of MitoSox-positive cells in vehicle with vehicle (Aa), rTNFα with vehicle (Ab), and rTNFα with Mito-T (Ac). Scale bar, 50 μm. ***B***, The effect of Mito-T on the MitoSox signals in the cultured B35 cells. MitoSox signals in the groups of vehicle + vehicle, rTNFα + vehicle, and rTNFα + Mito-T; ***$p < 0.001$ versus vehicle + vehicle; ###$p < 0.001$ versus rTNFα + vehicle; one-way ANOVA, *post hoc* PLSD test; $n = 3$. ***C***, The effect of Mito-T on pCREB in the cultured B35 cells treated with rTNFα; ***$p < 0.001$ versus vehicle + vehicle; ###$p < 0.001$ versus rTNFα + vehicle; one-way ANOVA, *post hoc* PLSD test; $n = 4$. ***D***, The effect of Mito-T on pC/EBPβ in the B35 cells treated with rTNFα; **$p < 0.01$ versus vehicle + vehicle; ##$p < 0.01$ versus rTNFα + vehicle; one-way ANOVA; $n = 4$. ***E***, The effect of Mito-T on C/EBPβ in the B35 cells treated with rTNFα; ***$p < 0.001$ versus vehicle + vehicle; ##$p < 0.01$ versus rTNFα + vehicle; one-way ANOVA; $n = 4$. ***F***, The effect of AS-CREB on pCREB in the B35 cells treated with rat rTNFα or vehicle; **$p < 0.01$ versus mmODN + vehicle; ##$p < 0.01$ versus mmODN + rTNFα; one-way ANOVA; $n = 3$. ***G***, The effect of AS-CREB on pC/EBPβ in the B35 cells; **$p < 0.01$ versus mmODN + vehicle; ##$p < 0.01$ versus mmODN + rTNFα; one-way ANOVA; $n = 3$. ***H***, AS-CREB on total C/EBPβ in the B35 cells; **$p < 0.01$ versus mmODN + vehicle; ###$p < 0.001$ versus mmODN + rTNFα; one-way ANOVA, $n = 3$. ***I***, The possible pathway in the rat neuronal B35 cells treated with rTNFα. TNFα triggered overproduction of mitochondrial superoxide. The oxidative stress induced pCREB. Furthermore, pCREB caused pC/EBPβ in the neuronal B35 cells.

cells. Western blots showed that AS-CREB reversed the upregulated pCREB (Fig. 9*F*). The expression of pC/EBPβ in the mmODN + rTNFα group was higher than that in the mmODN + vehicle ($p < 0.01$, one-way ANOVA *post hoc* PLSD test; Fig. 9*G*). There was a significant decrease in pC/EBPβ in the AS-CREB + rTNFα group compared with that in mmODN + rTNFα ($p < 0.01$, one-way ANOVA, *post hoc* PLSD test; Fig. 9*G*). Similarly, C/EBPβ in mmODN + TNFα group was higher than that in mmODN + vehicle; C/EBPβ was lowered in the AS-CREB + rTNFα group compared with that in mmODN + rTNFα (Fig. 9*H*), demonstrating that pC/EBPβ was the downstream factor of pCREB. Figure 9*I* shows rTNFα evokes $mtO_2^{\cdot-}$–pCREB–pC/EBPβ pathway in the cultured neurons.

Effect of intrathecal rTNFα on $mtO_2^{\cdot-}$, pCREB, and pC/EBPβ in *in vivo* study

To further confirm pC/EBPβ pathway induced by TNFα, we intrathecally injected rTNFα (0.3 ng, twice a day for 2 d) or saline (vehicle) to naive rats. At day 3, 16 h after the last injection of rTNFα, we found mechanical threshold decreased in rats with rTNFα compared with that in saline ($p < 0.01$ vs vehicle, *t* test; Fig. 10*A*), suggesting that repeated rTNFα alone induces neuropathic pain. At 16 h after the last rTNFα injection, we gave intrathecal MitoSox Red, and 70 min later perfused animals. The images of MitoSox in the SCDH were shown in Figure 10*B*. Intrathecal rTNFα increased MitoSox-positive cell number in the SCDH lamina I–II and III–V ($p < 0.001$ vs vehicle, *t* test; Fig.

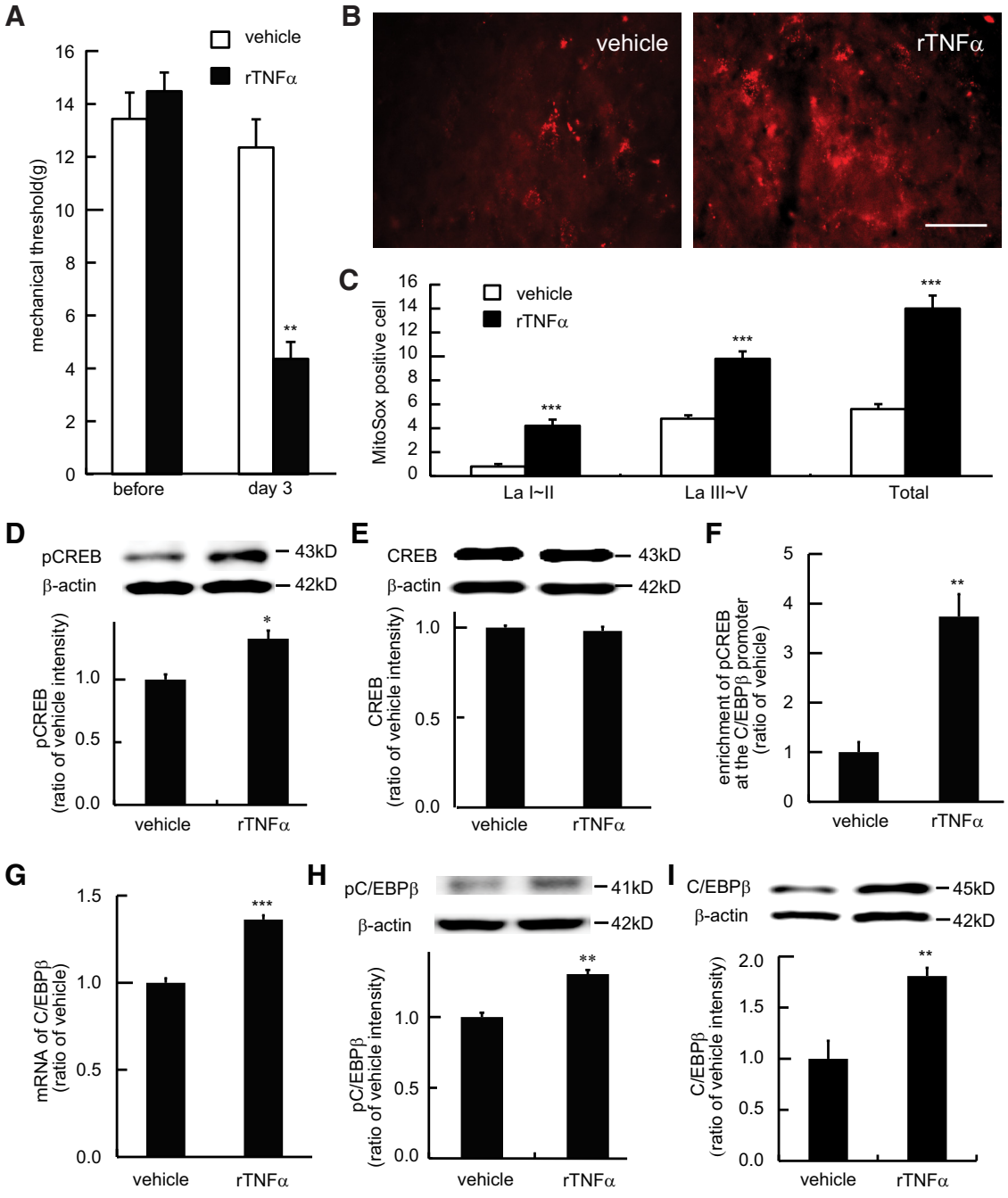

Figure 10. The effect of intrathecal rTNFα on mechanical threshold, MitoSox image, pCREB, and pC/EBPβ in naive rats. Intrathecal rTNFα (0.3 ng, twice a day for 2 d) or saline (vehicle) was administered. At day 3 (16 h post the last rTNFα), mechanical threshold was measured and the SCDH harvested. ***A***, Intrathecal rTNFα decreased mechanical threshold at day 3; $^{**}p < 0.01$ versus vehicle, *t* test; $n = 5$. ***B***, Representative imaging of MitoSox with vehicle or rTNFα. ***C***, Intrathecal rTNFα increased the number of MitoSox-positive cells in the SCDH lamina I–II and III–V ($^{***}p < 0.001$ vs vehicle, *t* test; $n = 5$). ***D***, Intrathecal rTNFα increased pCREB ($^{*}p < 0.05$ vs vehicle, *t* test; $n = 5$), but not total CREB ***E***, ***F***, ChIP-qPCR assay showed that intrathecal rTNFα increased the enrichment of pCREB on the C/EBPβ gene promoter regions compared with vehicle ($^{**}p < 0.01$ vs vehicle, *t* test; $n = 4–5$). ***G***, RT-PCR displayed that mRNA of C/EBPβ was increased by intrathecal rTNFα compared with vehicle ($^{***}p < 0.01$ vs vehicle, *t* test; $n = 5$). Western blots also showed an increase in pC/EBPβ (***H***) and C/EBPβ (***I***) induced by intrathecal rTNFα ($^{**}p < 0.01$ vs vehicle, *t* test; $n = 5$).

10*C*). In a separate setting of experiment, at 16 h after the last injection of rTNFα, we harvested the spinal cord. Western blots showed that intrathecal rTNFα increased pCREB ($p < 0.05$, *t* test; Fig. 10*D*), but not total CREB (Fig. 10*E*). ChIP-qPCR assay showed that intrathecal rTNFα increased the enrichment of pCREB on the C/EBPβ gene promoter regions compared with saline ($p < 0.01$ vs vehicle, *t* test; Fig. 10*F*). Intrathecal rTNFα increased the expression of mRNA of C/EBPβ compared with saline ($p < 0.001$ vs vehicle, *t* test; Fig. 10*G*). Western blots displayed that intrathecal rTNFα significantly upregulated pC/EBPβ (Fig. 10*H*) and C/EBPβ (Fig. 10*I*; $p < 0.01$ vs vehicle, *t* test).

Relationship of TNFα, $mtO_2^{\cdot-}$, pCREB, and pC/EBPβ in rats treated with intrathecally repeated rTNFα

Intrathecal Mito-T significantly increased mechanical threshold in rats treated with intrathecally repeated rTNFα, which lasted

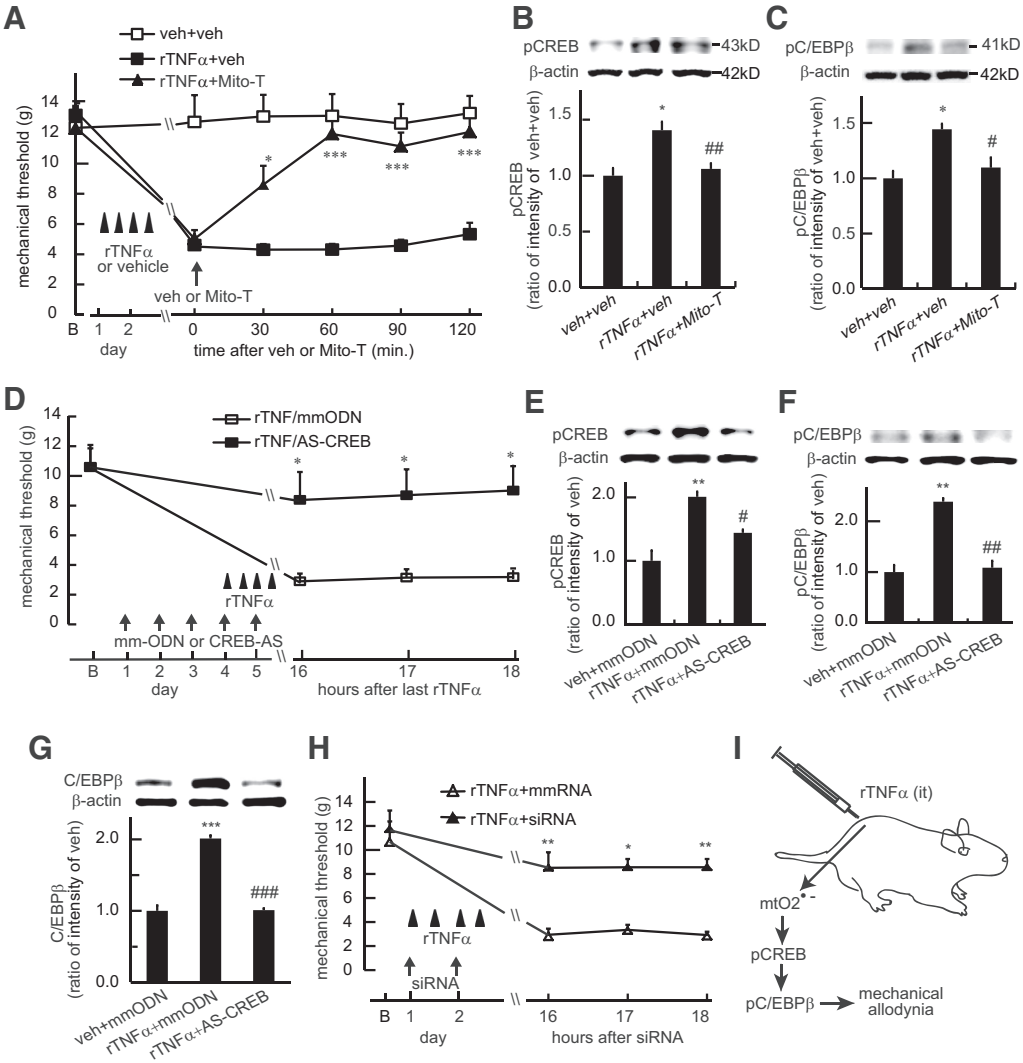

Figure 11. The relationship among $mtO_2^{\cdot-}$, pCREB, and pC/EBPβ in the SCDH in rats treated with intrathecal rTNFα. ***A***, Naive rats received intrathecal injection of saline (vehicle) or rTNFα (twice a day for 2 d; arrowhead). At day 3, 16 h post the last rTNFα injection, rats received intrathecal mitochondrial superoxide scavenger Mito-T or vehicle, and mechanical threshold was measured. The SCDH was harvested at 2 h after intrathecal compounds. Arrows showed vehicle or Mito-T injection. Intrathecal Mito-T significantly reversed mechanical threshold lowered by rTNFα; $F_{(10,70),\ \text{interaction}} = 9.54$, $p < 0.0001$; $F_{(5,70),\ \text{main effect time}} = 15.06$, $p < 0.0001$; $F_{(2,14),\ \text{main effect treatment}} = 13.81$, $p < 0.001$; two-way repeated-measures ANOVA; $n = 5$–7. Mechanical withdrawal threshold in the rTNFα+Mito-T group was higher than that in rTNFα+vehicle at 30–120 min; $^{*}p < 0.05$; $^{***}p < 0.001$ versus rTNFα+vehicle; two-way repeated-measures ANOVA with Bonferroni *post hoc* test; $n = 6$–7. ***B***, The effect of intrathecal Mito-T on pCREB in rats treated with rTNFα; $^{*}p < 0.05$ versus vehicle+vehicle group; $^{\#\#}p < 0.01$ versus rTNFα+vehicle group; one-way ANOVA, *post hoc* PLSD test; $n = 4$–5. ***C***, The effect of Mito-T on pC/EBPβ in rats treated with rTNFα; $^{*}p < 0.05$ versus vehicle+vehicle group; $^{\#}p < 0.05$ versus rTNFα+vehicle; one-way ANOVA; $n = 4$–5. ***D***, The effect of intrathecal AS-CREB on mechanical threshold in rats with rTNFα. Arrows show the ODN injections. AS-CREB significantly reversed the lowered mechanical threshold; $F_{(3,30),\ \text{interaction}} = 3.57$, $p < 0.05$; $F_{(3,30),\ \text{main effect time}} = 9.93$, $p < 0.001$; $F_{(1,11),\ \text{main effect treatment}} = 7.43$, $p < 0.05$; two-way repeated-measures ANOVA; $n = 6$. Mechanical withdrawal threshold in the rTNFα+AS-CREB group was higher than that in rTNFα+mmODN at 16–18 h after the last rTNFα; $^{*}p < 0.05$, two-way repeated-measures ANOVA with Bonferroni test; $n = 6$. ***E***, The effect of intrathecal AS-CREB on spinal pCREB in rat treated with rTNFα; $^{**}p < 0.01$ versus vehicle+mmODN; $^{\#}p < 0.05$ versus rTNFα+mmODN; one-way ANOVA; $n = 4$–5. ***F***, The effect of intrathecal AS-CREB on pC/EBPβ in rat treated with intrathecal rTNFα; $^{**}p < 0.01$ versus vehicle+mmODN; $^{\#\#}p < 0.01$ versus rTNFα+mmODN; one-way ANOVA; $n = 4$–5. ***G***, The effect of intrathecal AS-CREB on total C/EBPβ in rat treated with intrathecal rTNFα; $^{***}p < 0.001$ versus vehicle+mmODN; $^{\#\#\#}p < 0.001$ versus rTNFα+mmODN; one-way ANOVA; $n = 4$–5. ***H***, The effect of intrathecal C/EBPβ siRNA or mmRNA on mechanical threshold in rats with intrathecal rTNFα. Arrows show the siRNA injections. Intrathecal C/EBPβ siRNA significantly increased mechanical threshold compared with mmRNA; $F_{(3,24),\ \text{interaction}} = 3.19$, $p < 0.05$; $F_{(3,24),\ \text{main effect time}} = 18.31$, $p < 0.0001$; $F_{(1,8),\ \text{main effect treatment}} = 14.36$, $p < 0.01$; two-way repeated-measures ANOVA; $n = 5$. Mechanical withdrawal threshold in the rTNFα+siRNA group was higher than that in rTNFα+mmRNA at 16–18 h after the last rTNFα; $^{*}p < 0.05$, $^{**}p < 0.01$; two-way repeated-measures ANOVA with Bonferroni test; $n = 6$–7. ***I***, The possible pathway in rats treated with intrathecal rTNFα in naive rats. TNFα triggered mitochondrial oxidative stress inducing the phosphorylation of CREB, which furthermore induced pC/EBPβ. Phospho-C/EBPβ plays important role in the neuropathic pain state.

>2 h ($F_{(10,70),\ \text{interaction}} = 9.54$, $p < 0.0001$; $F_{(5,70),\ \text{main effect time}} = 15.06$, $p < 0.0001$; $F_{(2,14),\ \text{main effect treatment}} = 13.81$, $p < 0.001$; two-way repeated-measures ANOVA, $n = 5$–7 (Fig. 11*A*). Mechanical withdrawal threshold in the rTNFα+Mito-T group was significantly higher than that in rTNFα+vehicle at 30–120 min (two-way ANOVA, Bonferroni tests; Fig. 11*A*). Western blots displayed that pCREB in the rTNFα+vehicle group was higher than that in vehicle+ vehicle ($p < 0.05$, one-way ANOVA, *post hoc* PLSD test), and that there was a significant decrease in pCREB in the rTNFα+Mito-T compared with that in the rTNFα+ vehicle ($p < 0.01$, one-way ANOVA, *post hoc* PLSD test; Fig. 11*B*). Similarly, Mito-T decreased the upregulated pC/EBPβ (Fig. 11*C*), suggesting that pCREB and pC/EBPβ were mediated by $mtO_2^{\cdot-}$ in rats treated with repeated rTNFα *in vivo*.

To examine whether CREB was involved in the painful response triggered by intrathecal rTNFα, we proceeded to knockdown CREB by intrathecal AS-CREB. AS-CREB significantly reversed the lowered mechanical threshold ($F_{(3,30),\ \text{interaction}} = 3.57$, $p < 0.05$;

$F_{(3,30),\ \text{main effect time}} = 9.93$, $p < 0.001$; $F_{(1,11),\ \text{main effect treatment}} = 7.43$; $p < 0.05$, two-way repeated-measures ANOVA; $n = 6$; Fig. 11*D*). Mechanical threshold in the rTNFα+AS-CREB group was higher than that in rTNFα+mmODN at 16–18 h after the last rTNFα ($p < 0.05$, two-way ANOVA, Bonferroni tests; Fig. 11*D*). Western blots showed that pCREB in the rTNFα+mmODN group was higher than that in vehicle+mmODN ($p < 0.01$, one-way ANOVA, *post hoc* PLSD test), and that there was a significant decrease in pCREB in the rTNFα+AS-CREB compared with that in the rTNFα+mmODN ($p < 0.05$, one-way ANOVA, *post hoc* PLSD test; Fig. 11*E*). Similarly, antisense ODN against CREB decreased the upregulation of pC/EBPβ (Fig. 11*F*) and C/EBPβ (Fig. 11*G*), suggesting that pC/EBPβ were mediated by CREB signal in rats treated with repeated rTNFα *in vivo*.

To investigate whether C/EBPβ played a role in the painful behavior in rats with intrathecally repeated rTNFα, we knocked down the expression of C/EBPβ using C/EBPβ siRNA. Intrathecal C/EBPβ siRNA or mismatch siRNA was administered once a day for 2 d. Intrathecal C/EBPβ siRNA significantly increased mechanical threshold ($F_{(3,24),\ \text{interaction}} = 3.19$, $p < 0.05$; $F_{(3,24),\ \text{main effect time}} = 18.31$, $p < 0.0001$; $F_{(1,8),\ \text{main effect treatment}} = 14.36$, $p < 0.01$, two-way repeated-measures ANOVA; $n = 5$; Fig. 11*H*). Mechanical withdrawal threshold in the rTNFα+siRNA group was higher than that in rTNFα+mmRNA at 16–18 h after the last rTNFα (two-way ANOVA Bonferroni tests; Fig. 11*H*). Figure 11*I* shows that intrathecal rTNFα may evoke $mtO_2^{\cdot-}$–pCREB–pC/EBPβ in rats.

Discussion

The mechanisms underlying HIV-associated chronic pain remain unclear. C/EBPβ has been shown to be a critical transcriptional regulator of HIV-1, and influences AIDS progression (Mameli et al., 2007). Our data demonstrate that spinal pC/EBPβ triggered by TNFα/TNFRI–$mtO_2^{\cdot-}$–pCREB pathway, is involved in the peripheral gp120-induced neuropathic pain. Furthermore, in *in vitro* studies, using the cultured neuronal cells, we show that treatment with rTNFα to the cultured neurons, induced the $mtO_2^{\cdot-}$–pCREB–pC/EBPβ pathway; intrathecal rTNFα administration evoked the same pathway in naive rats.

C/EBPβ expression has been observed in a variety of primary neuronal cultures and neuronal cell lines, cultured astrocytes, and microglia (Pulido-Salgado et al., 2015). In *in vivo* studies, C/EBPβ immunoreactivity after systemic LPS colocalizes with markers of endothelial cells, neurons, astrocytes, and microglia depending on the brain areas (Damm et al., 2011; Fuchs et al., 2013). In the present study, we found that peripheral gp120 application onto the sciatic nerve induced the expression of pC/EBPβ in the neurons of the spinal cord dorsal horn. pC/EBPβ may influence AIDS progression by increasing expression of HIV-1 genes (Mameli et al., 2007). The expression of C/EBPβ mRNA is elevated and its protein is expressed in the brain of HIV-1-infected and HIV-1 encephalitis patients (Fields et al., 2011). Evidence from *in vitro* studies show that C/EBPβ is activated by TNFα in cultured macrophages (Portillo et al., 2012). Painful HIV-associated sensory neuropathy is a neurological complication of HIV infection. However, it is unclear about the exact molecular mechanisms and signal pathways of pC/EBPβ in HIV-related pain.

The cellular mechanisms by which peripheral gp120 onto the sciatic nerve induces neuropathic pain are still not clear. HIV rarely induces neuronal infection, thus, neurotoxicity may be induced by secreted HIV proteins, such as gp120 in the pathogenesis of HIV-sensory neuropathy via chemokine receptors (Kaul et al., 2001; Keswani et al., 2003; Liu et al., 2015). Keswani et al. (2003)report that C-X-C chemokine receptor type 4 (CXCR4; an HIV coreceptor) on Schwann cells by gp120 results in the release of RANTES, which induces TNFα production in cultured DRG sensory neurons, leading to subsequent TNFR1-mediated neurotoxicity in an autocrine/paracrine fashion. We and others report that in *in vivo* studies, the gp120-exposed sciatic nerve increases TNFα within the nerve trunk (Herzberg and Sagen, 2001) and DRG (Zheng et al., 2011; Hao, 2013). HIV gp120 induces upregulation of CXCR4 and stromal cell-derived factor-1α (SDF1-α) in both the DRG and SCDH (Huang et al., 2014). Anti-inflammatory IL-10 reversed the upregulation of TNFα, SDF-1α, and CXCR4 in the DRG (Zheng et al., 2014). Peripheral inflammation induces the hyperfunction of nociceptive transduction ion channels on the sensory neurons (Yekkirala et al., 2017), leading to a reduction in the threshold for activation and hyperexcitability of nociceptor sensory neurons (Costigan et al., 2009). A prolonged increase in excitability and synaptic efficacy of central nociceptive neurons is partially driven by activity in peripheral nociceptors as a form of activity-dependent plasticity (Yekkirala et al., 2017). On persistent activation of nociceptive primary afferent input to the spinal cord, activated astrocytes and microglia release a number of signaling molecules (for example, TNFα; Herzberg and Sagen, 2001; Wallace et al., 2007b), which play important role in inflammatory and neuropathic pain (Milligan and Watkins, 2009; Grace et al., 2014). HIV-1 transgenic rats overexpressing gp120 induce reactive gliosis in brain (Reid et al., 2001). Indeed, intrathecal gp120 induces an acute painful behavior and proinflammatory cytokine release in the spinal cord (Milligan et al., 2001). CSF from patients with AIDS shows an increase in TNFα (Tyor et al., 1992). TNFα has also been implicated in the pathogenesis of HIV-1 infection, promoting HIV replication in T cell lines and in lymphocytes in HIV-infected patients (Cepeda et al., 2008). Serum TNFα has been shown to increase as HIV-1 infection progresses (Aukrust et al., 1994), suggesting that TNFα may contribute to disease progression. We have reported that gp120 application onto the sciatic nerve decreases mechanical threshold, and induces spinal glial activity releasing TNFα in the SCDH; intrathecal TNFα siRNA or recombinant TNFSR reduces gp120-induced mechanical allodynia (Zheng et al., 2011). In the present studies, we found that TNFRI was expressed on the neurons of the SCDH (Fig. 2). Thus, it is possible that glial TNFα activate neurons through TNFRI. The downstream signal of TNFRI in the HIV neuropathic pain is still not clear. TNFR1 constitutively forms a complex with endogenous c-Src and Jak2 kinases, and phosphatidylinositol 3-kinase (PI3K) to engage signaling cascades, activate transcription factors, and alter gene expression in *in vitro* studies (Pincheira et al., 2008). PI3K promotes recruitment of Akt to the plasma membrane and its subsequent activation (Cantley, 2002). PI3K-Akt activation is associated with the accumulation of mitochondrial ROS (Hamanaka and Chandel, 2010).

Oxidative stress causes activation of a number of complex and interrelated signaling events (Chandra et al., 2000). Recent work shows that ROS are involved in the development and maintenance of neuropathic pain. Removal of excessive ROS by free radical scavengers, such as phenyl *N*-*tert*-butylnitrone and 4-hydroxy-2, 2,6,6-tetramethylpiperidine 1-oxyl, produced a significant analgesic effect in both neuropathic and inflammatory pain (Gao et al., 2007; Fidanboylu et al., 2011). In contrast, intrathecal ROS donor, *tert*-butyl hydroperoxide, produces transient pain behaviors in naive mice (Schwartz et al., 2008). Mitochondrial oxidative stress causes activation of a number of complex and interrelated

signaling events in the pathogenesis of chronic pain (Sui et al., 2013). Furthermore, $mtO_2^{\cdot-}$ accumulation was observed primarily in the mitochondria of SCDH neurons in different pain models (Schwartz et al., 2008, 2009; Kim et al., 2011). HIV gp120 has been implicated in initiation and/or intensification of ROS (Perl and Banki, 2000). In the present studies, we demonstrate that gp120 application increased spinal $mtO_2^{\cdot-}$. From *in vitro* and *in vivo* results of the current studies, blockage of TNFα bioactivity using rTNFSR reduced the $mtO_2^{\cdot-}$ in the SCDH neurons, indicating that TNFα-TNFRI activity in neurons induced the $mtO_2^{\cdot-}$ overexpression.

Previous studies have shown the various effects of ROS leading to activation of intracellular protein phosphorylation during spinal neuronal synaptic plasticity (Kim et al., 2011). Altered transcriptional factors are involved in chronic pain conditions (Ma et al., 2003). In response to neural activity or tissue inflammation, phosphorylation of CREB induces the expression of genes, which results in long-lasting synaptic plasticity (Nestler, 2002; Carlezon et al., 2005; Hagiwara et al., 2009). Nociceptor afferents activation contributes to central sensitization through CREB-mediated transcriptional regulation in the SCDH neurons (Kawasaki et al., 2004). Intrathecal CREB-antisense oligonucleotide attenuates neuropathic or inflammatory pain (Ma et al., 2003; Gu et al., 2013; Ferrari et al., 2015a,b), suggesting that spinal pCREB may contribute to the development of chronic pain (Gu et al., 2013). Recent studies show that pCREB is upregulated in the SCDH of pain-positive HIV patients (Shi et al., 2012). The current results showed that gp120 application onto the sciatic nerve increased the expression of spinal pCREB and that rTNFα application increased the expression of pCREB in *in vitro* and *in vivo* studies. The overexpression of pCREB was blocked by Mito-T, suggesting $mtO_2^{\cdot-}$ mediated pCREB (a downstream factor of mitochondrial superoxide).

The functional activation of CREB leads to the expression of target genes including the transcription factor C/EBP presumably regulating the expression of a late response gene (for review, see Alberini, 2009). There is a cooperative interaction between CREB and C/EBPβ in human T cells treated with PGE2 (Dumais et al., 2002). The increase in pC/EBP is considered a correlate of the relative extent of long-term facilitation (Liu et al., 2013). The expression of constitutively active CREB strongly activates C/EBPβ promoter, and induces the expression of endogenous C/EBPβ in preadipocyte cells (Zhang et al., 2004). Learning-induced increases in the hippocampal C/EBPβ expression are CREB-dependent (Athos et al., 2002). Using ChIP assay we observed that pCREB bound C/EBPβ promoter. In our *in vitro* and *in vivo* studies, knockdown of CREB using CREB antisense ODN increased mechanical threshold, and reduced the expression of C/EBPβ and pC/EBPβ, indicating that C/EBPβ/pC/EBPβ is mediated by CREB phosphorylation in the epigenetic level.

The relationships among $mtO_2^{\cdot-}$, pCREB, and pC/EBPβ are not clear yet. It is possible that a positive feedback circuit with pCREB is involved in their interactions. Phosphorylated CREB leads to C/EBP presumably regulating the expression of a late response gene (for review, see Alberini, 2009). C/EBPβ regulates sorting nexin 27 (SNX27, regulating endocytic sorting and trafficking), which promotes recycling of NMDA receptors from endosomes to the plasma membrane (Wang et al., 2013). NMDA receptors increase Ca^{2+} influx (Ohno et al., 2002; Valnegri et al., 2015). HIV gp120 stimulates a rapid increase in intracellular free Ca^{2+} accumulation in the dorsal horn cells of the mice spinal cord (Minami et al., 2003). Spinal cytosolic Ca^{2+} concentration contributes to the painful neuropathy (Sanna et al., 2015). Mitochondria are the major sites of ROS production in neurons, and participate in the regulation of cellular Ca^{2+} homeostasis (Camello-Almaraz et al., 2006; Kann and Kovács, 2007; Douda et al., 2015). There is an interaction of cytosolic Ca^{2+} and mitochondrial ROS generation (Kann and Kovács, 2007; Korbecki et al., 2013; Douda et al., 2015). NMDA activity-induced CaMKinase signaling contributes to CREB-dependent transcription (Impey et al., 2002). Thus we think, it is highly possible that positive feedback pathway of pCREB–ROS–pCREB through NMDA/Ca^{2+} is involved in the gp120 neuropathic pain state. In the near future studies, we will examine the exact role of NMDA/Ca^{2+} in the positive feedback pathway.

In summary, to our knowledge, we are the first to demonstrate that the expression of pC/EBPβ is triggered by the TNFα/TNFRI–$mtO_2^{\cdot-}$–pCREB pathway in peripheral gp120-induced neuropathic pain, which is supported by our *in vitro* studies in the cultured neuronal cells and intrathecal rTNFα administration in naive rats. This finding provides new insights in the understanding of the HIV neuropathic pain mechanisms and also suggests additional potential targets for successful treatment.

References

Ahmed KA, Sawa T, Ihara H, Kasamatsu S, Yoshitake J, Rahaman MM, Okamoto T, Fujii S, Akaike T (2012) Regulation by mitochondrial superoxide and NADPH oxidase of cellular formation of nitrated cyclic GMP: potential implications for ROS signalling. Biochem J 441:719–730. CrossRef Medline

Alberini CM (2009) Transcription factors in long-term memory and synaptic plasticity. Physiol Rev 89:121–145. CrossRef Medline

Athos J, Impey S, Pineda VV, Chen X, Storm DR (2002) Hippocampal CRE-mediated gene expression is required for contextual memory formation. Nat Neurosci 5:1119–1120. CrossRef Medline

Aukrust P, Liabakk NB, Müller F, Lien E, Espevik T, Frøland SS (1994) Serum levels of tumor necrosis factor-alpha (TNF alpha) and soluble TNF receptors in human immunodeficiency virus type 1 infection: correlations to clinical, immunologic, and virologic parameters. J Infect Dis 169:420–424. CrossRef Medline

Brookheart RT, Michel CI, Listenberger LL, Ory DS, Schaffer JE (2009) The non-coding RNA gadd7 is a regulator of lipid-induced oxidative and endoplasmic reticulum stress. J Biol Chem 284:7446–7454. CrossRef Medline

Camello-Almaraz C, Gomez-Pinilla PJ, Pozo MJ, Camello PJ (2006) Mitochondrial reactive oxygen species and Ca^{2+} signaling. Am J Physiol Cell Physiol 291:C1082–1088. CrossRef Medline

Cantley LC (2002) The phosphoinositide 3-kinase pathway. Science 296:1655–1657. CrossRef Medline

Carlezon WA Jr, Duman RS, Nestler EJ (2005) The many faces of CREB. Trends Neurosci 28:436–445. CrossRef Medline

Cepeda EJ, Williams FM, Ishimori ML, Weisman MH, Reveille JD (2008) The use of anti-tumour necrosis factor therapy in HIV-positive individuals with rheumatic disease. Ann Rheum Dis 67:710–712. CrossRef Medline

Chandra J, Samali A, Orrenius S (2000) Triggering and modulation of apoptosis by oxidative stress. Free Radic Biol Med 29:323–333. CrossRef Medline

Chaplan SR, Bach FW, Pogrel JW, Chung JM, Yaksh TL (1994) Quantitative assessment of tactile allodynia in the rat paw. J Neurosci Methods 53:55–63. CrossRef Medline

Cherry CL, Wadley AL, Kamerman PR (2012) Painful HIV-associated sensory neuropathy. Pain Management 2:543–552. CrossRef Medline

Costigan M, Scholz J, Woolf CJ (2009) Neuropathic pain: a maladaptive response of the nervous system to damage. Annu Rev Neurosci 32:1–32. CrossRef Medline

Damm J, Luheshi GN, Gerstberger R, Roth J, Rummel C (2011) Spatiotemporal nuclear factor interleukin-6 expression in the rat brain during lipopolysaccharide-induced fever is linked to sustained hypothalamic inflammatory target gene induction. J Comp Neurol 519:480–505. CrossRef Medline

Douda DN, Khan MA, Grasemann H, Palaniyar N (2015) SK3 channel and mitochondrial ROS mediate NADPH oxidase-independent NETosis

induced by calcium influx. Proc Natl Acad Sci U S A 112:2817–2822. CrossRef Medline

Dumais N, Bounou S, Olivier M, Tremblay MJ (2002) Prostaglandin E(2)-mediated activation of HIV-1 long terminal repeat transcription in human T cells necessitates CCAAT/enhancer binding protein (C/EBP) binding sites in addition to cooperative interactions between C/EBPbeta and cyclic adenosine 5′-monophosphate response element binding protein. J Immunol 168:274–282. CrossRef Medline

Ferrari LF, Bogen O, Reichling DB, Levine JD (2015a) Accounting for the delay in the transition from acute to chronic pain: axonal and nuclear mechanisms. J Neurosci 35:495–507. CrossRef Medline

Ferrari LF, Araldi D, Levine JD (2015b) Distinct terminal and cell body mechanisms in the nociceptor mediate hyperalgesic priming. J Neurosci 35:6107–6116. CrossRef Medline

Fidanboylu M, Griffiths LA, Flatters SJ (2011) Global inhibition of reactive oxygen species (ROS) inhibits paclitaxel-induced painful peripheral neuropathy. PloS One 6:e25212. CrossRef Medline

Fields J, Gardner-Mercer J, Borgmann K, Clark I, Ghorpade A (2011) CCAAT/enhancer binding protein beta expression is increased in the brain during HIV-1-infection and contributes to regulation of astrocyte tissue inhibitor of metalloproteinase-1. J Neurochem 118:93–104. CrossRef Medline

Fuchs F, Damm J, Gerstberger R, Roth J, Rummel C (2013) Activation of the inflammatory transcription factor nuclear factor interleukin-6 during inflammatory and psychological stress in the brain. J Neuroinflammation 10:140. CrossRef Medline

Gao X, Kim HK, Chung JM, Chung K (2007) Reactive oxygen species (ROS) are involved in enhancement of NMDA-receptor phosphorylation in animal models of pain. Pain 131:262–271. CrossRef Medline

Grace PM, Hutchinson MR, Maier SF, Watkins LR (2014) Pathological pain and the neuroimmune interface. Nat Rev Immunol 14:217–231. CrossRef Medline

Gu X, Bo J, Zhang W, Sun X, Zhang J, Yang Y, Ma Z (2013) Intrathecal administration of cyclic AMP response element-binding protein-antisense oligonucleotide attenuates neuropathic pain after peripheral nerve injury and decreases the expression of *N*-methyl-D-aspartic receptors in mice. Oncol Rep 30:391–398. CrossRef Medline

Hagiwara H, Ishida M, Arita J, Mitsushima D, Takahashi T, Kimura F, Funabashi T (2009) The cAMP response element-binding protein in the bed nucleus of the stria terminalis modulates the formalin-induced pain behavior in the female rat. Eur J Neurosci 30:2379–2386. CrossRef Medline

Hamanaka RB, Chandel NS (2010) Mitochondrial reactive oxygen species regulate cellular signaling and dictate biological outcomes. Trends Biochem Sci 35:505–513. CrossRef Medline

Hao S (2013) The molecular and pharmacological mechanisms of HIV-related neuropathic pain. Curr Neuropharmacol 11:499–512. CrossRef Medline

Hao S, Liu S, Zheng X, Zheng W, Ouyang H, Mata M, Fink DJ (2011) The role of TNFα in the periaqueductal gray during naloxone-precipitated morphine withdrawal in rats. Neuropsychopharmacology 36:664–676. CrossRef Medline

Heller EA, Hamilton PJ, Burek DD, Lombroso SI, Peña CJ, Neve RL, Nestler EJ (2016) Targeted epigenetic remodeling of the *Cdk5* gene in nucleus accumbens regulates cocaine- and stress-evoked behavior. J Neurosci 36:4690–4697. CrossRef Medline

Herzberg U, Sagen J (2001) Peripheral nerve exposure to HIV viral envelope protein gp120 induces neuropathic pain and spinal gliosis. J Neuroimmunol 116:29–39. CrossRef Medline

Hoefer MM, Sanchez AB, Maung R, de Rozieres CM, Catalan IC, Dowling CC, Thaney VE, Piña-Crespo J, Zhang D, Roberts AJ, Kaul M (2015) Combination of methamphetamine and HIV-1 gp120 causes distinct long-term alterations of behavior, gene expression, and injury in the central nervous system. Exp Neurol 263:221–234. CrossRef Medline

Höke A, Cornblath DR (2004) Peripheral neuropathies in human immunodeficiency virus infection. Suppl Clin Neurophysiol 57:195–210. CrossRef Medline

Huang W, Zheng W, Liu S, Zeng W, Levitt RC, Candiotti KA, Lubarsky DA, Hao S (2014) HSV-mediated p55TNFSR reduces neuropathic pain induced by HIV gp120 in rats through CXCR4 activity. Gene Ther 21:328–336. CrossRef Medline

Iida T, Yi H, Liu S, Huang W, Kanda H, Lubarsky DA, Hao S (2016) Spinal CPEB-mtROS-CBP signaling pathway contributes to perineural HIV gp120 with ddC-related neuropathic pain in rats. Exp Neurol 281:17–27. CrossRef Medline

Imai S, Ikegami D, Yamashita A, Shimizu T, Narita M, Niikura K, Furuya M, Kobayashi Y, Miyashita K, Okutsu D, Kato A, Nakamura A, Araki A, Omi K, Nakamura M, James Okano H, Okano H, Ando T, Takeshima H, Ushijima T, et al. (2013) Epigenetic transcriptional activation of monocyte chemotactic protein 3 contributes to long-lasting neuropathic pain. Brain 136:828–843. CrossRef Medline

Impey S, Fong AL, Wang Y, Cardinaux JR, Fass DM, Obrietan K, Wayman GA, Storm DR, Soderling TR, Goodman RH (2002) Phosphorylation of CBP mediates transcriptional activation by neural activity and CaM kinase IV. Neuron 34:235–244. CrossRef Medline

Jiang BC, He LN, Wu XB, Shi H, Zhang WW, Zhang ZJ, Cao DL, Li CH, Gu J, Gao YJ (2017) Promoted interaction of C/EBPα with demethylated *Cxcr3* gene promoter contributes to neuropathic pain in mice. J Neurosci 37:685–700. CrossRef Medline

Kanao M, Kanda H, Huang W, Liu S, Yi H, Candiotti KA, Lubarsky DA, Levitt RC, Hao S (2015) Gene transfer of glutamic acid decarboxylase 67 by herpes simplex virus vectors suppresses neuropathic pain induced by human immunodeficiency virus gp120 combined with ddC in rats. Anesth Analg 120:1394–1404. CrossRef Medline

Kanda H, Kanao M, Liu S, Yi H, Iida T, Levitt RC, Candiotti KA, Lubarsky DA, Hao S (2016a) HSV vector-mediated GAD67 suppresses neuropathic pain induced by perineural HIV gp120 in rats through inhibition of ROS and Wnt5a. Gene Ther 23:340–348. CrossRef Medline

Kanda H, Liu S, Iida T, Yi H, Huang W, Levitt RC, Lubarsky DA, Candiotti KA, Hao S (2016b) Inhibition of mitochondrial fission protein reduced mechanical allodynia and suppressed spinal mitochondrial superoxide induced by perineural HIV gp120 in rats. Anesth Analg 122:264–272. CrossRef Medline

Kann O, Kovács R (2007) Mitochondria and neuronal activity. Am J Physiol Cell Physiol 292:C641–657. Medline

Kaul M, Garden GA, Lipton SA (2001) Pathways to neuronal injury and apoptosis in HIV-associated dementia. Nature 410:988–994. CrossRef Medline

Kawasaki Y, Kohno T, Zhuang ZY, Brenner GJ, Wang H, Van Der Meer C, Befort K, Woolf CJ, Ji RR (2004) Ionotropic and metabotropic receptors, protein kinase A, protein kinase C, and Src contribute to C-fiber-induced ERK activation and cAMP response element-binding protein phosphorylation in dorsal horn neurons, leading to central sensitization. J Neurosci 24:8310–8321. CrossRef Medline

Keswani SC, Pardo CA, Cherry CL, Hoke A, McArthur JC (2002) HIV-associated sensory neuropathies. Aids 16:2105–2117. CrossRef Medline

Keswani SC, Polley M, Pardo CA, Griffin JW, McArthur JC, Hoke A (2003) Schwann cell chemokine receptors mediate HIV-1 gp120 toxicity to sensory neurons. Ann Neurol 54:287–296. CrossRef Medline

Kim HY, Lee KY, Lu Y, Wang J, Cui L, Kim SJ, Chung JM, Chung K (2011) Mitochondrial Ca^{2+} uptake is essential for synaptic plasticity in pain. J Neurosci 31:12982–12991. CrossRef Medline

Korbecki J, Baranowska-Bosiacka I, Gutowska I, Chlubek D (2013) The effect of reactive oxygen species on the synthesis of prostanoids from arachidonic acid. J Physiol Pharmacol 64:409–421. Medline

Kranick SM, Nath A (2012) Neurologic complications of HIV-1 infection and its treatment in the era of antiretroviral therapy. Continuum 18:1319–1337. CrossRef Medline

Lee KM, Jeon SM, Cho HJ (2009) Tumor necrosis factor receptor 1 induces interleukin-6 upregulation through NF-kappaB in a rat neuropathic pain model. Eur J Pain 13:794–806. CrossRef Medline

Liang Y, Harris FL, Brown LA (2014) Alcohol induced mitochondrial oxidative stress and alveolar macrophage dysfunction. Biomed Res Int 2014:371593. CrossRef Medline

Li Z, Mao Y, Liang L, Wu S, Yuan J, Mo K, Cai W, Mao Q, Cao J, Bekker A, Zhang W, Tao YX (2017) The transcription factor C/EBPβ in the dorsal root ganglion contributes to peripheral nerve trauma-induced nociceptive hypersensitivity. Sci Signal 10:eaam5345. CrossRef Medline

Liu CH, Godai K, Liu S, Levitt RC, Candiotti KA, Lubarsky DA, Hao S (2015) Prolonged intrathecal exposure to gp120 induces HIV-related neuropathic pain and spinal pharmacological characteristics. J Neuroimmune Pharmacol 10:S83.

Liu RY, Zhang Y, Baxter DA, Smolen P, Cleary LJ, Byrne JH (2013) Deficit in long-term synaptic plasticity is rescued by a computationally predicted stimulus protocol. J Neurosci 33:6944–6949. CrossRef Medline

Ma W, Hatzis C, Eisenach JC (2003) Intrathecal injection of cAMP response element binding protein (CREB) antisense oligonucleotide attenuates tactile allodynia caused by partial sciatic nerve ligation. Brain Res 988:97–104. CrossRef Medline

Mameli G, Deshmane SL, Ghafouri M, Cui J, Simbiri K, Khalili K, Mukerjee R, Dolei A, Amini S, Sawaya BE (2007) C/EBPβ regulates human immunodeficiency virus 1 gene expression through its association with cdk9. J Gen Virol 88:631–640. CrossRef Medline

Meeker RB, Poulton W, Clary G, Schriver M, Longo FM (2016) Novel p75 neurotrophin receptor ligand stabilizes neuronal calcium, preserves mitochondrial movement and protects against HIV associated neuropathogenesis. Exp neurol 275:182–198. CrossRef Medline

Merlin JS, Cen L, Praestgaard A, Turner M, Obando A, Alpert C, Woolston S, Casarett D, Kostman J, Gross R, Frank I (2012) Pain and physical and psychological symptoms in ambulatory HIV patients in the current treatment era. J Pain Symptom Manage 43:638–645. CrossRef Medline

Milligan ED, Watkins LR (2009) Pathological and protective roles of glia in chronic pain. Nat Rev Neurosci 10:23–36. CrossRef Medline

Milligan ED, O'Connor KA, Nguyen KT, Armstrong CB, Twining C, Gaykema RP, Holguin A, Martin D, Maier SF, Watkins LR (2001) Intrathecal HIV-1 envelope glycoprotein gp120 induces enhanced pain states mediated by spinal cord proinflammatory cytokines. J Neurosci 21:2808–2819. Medline

Minami T, Matsumura S, Mabuchi T, Kobayashi T, Sugimoto Y, Ushikubi F, Ichikawa A, Narumiya S, Ito S (2003) Functional evidence for interaction between prostaglandin EP3 and kappa-opioid receptor pathways in tactile pain induced by human immunodeficiency virus type-1 (HIV-1) glycoprotein gp120. Neuropharmacology 45:96–105. CrossRef Medline

Nath A (2015) Neurologic complications of human immunodeficiency virus infection. Continuum 21:1557–1576. CrossRef Medline

Nestler EJ (2002) Common molecular and cellular substrates of addiction and memory. Neurobiol Learn Mem 78:637–647. CrossRef Medline

Ohno M, Frankland PW, Silva AJ (2002) A pharmacogenetic inducible approach to the study of NMDA/αCaMKII signaling in synaptic plasticity. Curr Biol 12:654–656. CrossRef Medline

Perl A, Banki K (2000) Genetic and metabolic control of the mitochondrial transmembrane potential and reactive oxygen intermediate production in HIV disease. Antioxid Redox Signal 2:551–573. CrossRef Medline

Pincheira R, Castro AF, Ozes ON, Idumalla PS, Donner DB (2008) Type 1 TNF receptor forms a complex with and uses Jak2 and c-Src to selectively engage signaling pathways that regulate transcription factor activity. J Immunol 181:1288–1298. CrossRef Medline

Portillo JA, Feliciano LM, Okenka G, Heinzel F, Subauste MC, Subauste CS (2012) CD40 and tumour necrosis factor-alpha co-operate to upregulate inducible nitric oxide synthase expression in macrophages. Immunology 135:140–150. CrossRef Medline

Pulido-Salgado M, Vidal-Taboada JM, Saura J (2015) C/EBPβ and C/EBPδ transcription factors: basic biology and roles in the CNS. Prog Neurobiol 132:1–33. CrossRef Medline

Reid W, Sadowska M, Denaro F, Rao S, Foulke J Jr, Hayes N, Jones O, Doodnauth D, Davis H, Sill A, O'Driscoll P, Huso D, Fouts T, Lewis G, Hill M, Kamin-Lewis R, Wei C, Ray P, Gallo RC, Reitz M, et al. (2001) An HIV-1 transgenic rat that develops HIV-related pathology and immunologic dysfunction. Proc Natl Acad Sci U S A 98:9271–9276. CrossRef Medline

Salvemini D, Little JW, Doyle T, Neumann WL (2011) Roles of reactive oxygen and nitrogen species in pain. Free Radic Biol Med 51:951–966. CrossRef Medline

Samji H, Cescon A, Hogg RS, Modur SP, Althoff KN, Buchacz K, Burchell AN, Cohen M, Gebo KA, Gill MJ, Justice A, Kirk G, Klein MB, Korthuis PT, Martin J, Napravnik S, Rourke SB, Sterling TR, Silverberg MJ, Deeks S, et al. (2013) Closing the gap: increases in life expectancy among treated HIV-positive individuals in the United States and Canada. PloS One 8:e81355. CrossRef Medline

Sanna MD, Peroni D, Quattrone A, Ghelardini C, Galeotti N (2015) Spinal RyR2 pathway regulated by the RNA-binding protein HuD induces pain hypersensitivity in antiretroviral neuropathy. Exp Neurol 267:53–63. CrossRef Medline

Schwartz ES, Lee I, Chung K, Chung JM (2008) Oxidative stress in the spinal cord is an important contributor in capsaicin-induced mechanical secondary hyperalgesia in mice. Pain 138:514–524. CrossRef Medline

Schwartz ES, Kim HY, Wang J, Lee I, Klann E, Chung JM, Chung K (2009) Persistent pain is dependent on spinal mitochondrial antioxidant levels. J Neurosci 29:159–168. CrossRef Medline

Shi Y, Gelman BB, Lisinicchia JG, Tang SJ (2012) Chronic-pain-associated astrocytic reaction in the spinal cord dorsal horn of human immunodeficiency virus-infected patients. J Neurosci 32:10833–10840. CrossRef Medline

Sui BD, Xu TQ, Liu JW, Wei W, Zheng CX, Guo BL, Wang YY, Yang YL (2013) Understanding the role of mitochondria in the pathogenesis of chronic pain. Postgrad Med J 89:709–714. CrossRef Medline

Taubenfeld SM, Milekic MH, Monti B, Alberini CM (2001) The consolidation of new but not reactivated memory requires hippocampal C/EBP-beta. Nat Neurosci 4:813–818. CrossRef Medline

Tyor WR, Glass JD, Griffin JW, Becker PS, McArthur JC, Bezman L, Griffin DE (1992) Cytokine expression in the brain during the acquired immunodeficiency syndrome. Ann Neurol 31:349–360. CrossRef Medline

Valnegri P, Puram SV, Bonni A (2015) Regulation of dendrite morphogenesis by extrinsic cues. Trends Neurosci 38:439–447. CrossRef Medline

Wallace VC, Blackbeard J, Segerdahl AR, Hasnie F, Pheby T, McMahon SB, Rice AS (2007a) Characterization of rodent models of HIV-gp120 and anti-retroviral-associated neuropathic pain. Brain 130:2688–2702. CrossRef Medline

Wallace VC, Blackbeard J, Pheby T, Segerdahl AR, Davies M, Hasnie F, Hall S, McMahon SB, Rice AS (2007b) Pharmacological, behavioural and mechanistic analysis of HIV-1 gp120 induced painful neuropathy. Pain 133:47–63. CrossRef Medline

Wang X, Zhao Y, Zhang X, Badie H, Zhou Y, Mu Y, Loo LS, Cai L, Thompson RC, Yang B, Chen Y, Johnson PF, Wu C, Bu G, Mobley WC, Zhang D, Gage FH, Ranscht B, Zhang YW, Lipton SA, et al. (2013) Loss of sorting nexin 27 contributes to excitatory synaptic dysfunction by modulating glutamate receptor recycling in Down's syndrome. Nat Med 19:473–480. CrossRef Medline

Yekkirala AS, Roberson DP, Bean BP, Woolf CJ (2017) Breaking barriers to novel analgesic drug development. Nat Rev Drug Discov 16:545–564. CrossRef Medline

Yuan SB, Shi Y, Chen J, Zhou X, Li G, Gelman BB, Lisinicchia JG, Carlton SM, Ferguson MR, Tan A, Sarna SK, Tang SJ (2014) Gp120 in the pathogenesis of human immunodeficiency virus-associated pain. Ann Neurol 75:837–850. CrossRef Medline

Zhang JW, Klemm DJ, Vinson C, Lane MD (2004) Role of CREB in transcriptional regulation of CCAAT/enhancer-binding protein beta gene during adipogenesis. J Biol Chem 279:4471–4478. CrossRef Medline

Zheng W, Ouyang H, Zheng X, Liu S, Mata M, Fink DJ, Hao S (2011) Glial TNFα in the spinal cord regulates neuropathic pain induced by HIV gp120 application in rats. Mol Pain 7:40. CrossRef Medline

Zheng W, Huang W, Liu S, Levitt RC, Candiotti KA, Lubarsky DA, Hao S (2014) Interleukin 10 mediated by herpes simplex virus vectors suppresses neuropathic pain induced by human immunodeficiency virus gp120 in rats. Anesth Analg 119:693–701. CrossRef Medline

Zheng X, Zheng W, Liu S, Patel HM, Xia X, Ouyang H, Levitt RC, Candiotti KA, Hao S (2012) Crosstalk between JNK and NF-κB in the KDO2-mediated production of TNFα in HAPI cells. Cell Mol Neurobiol 32:1375–1383. CrossRef Medline